HELSINKI UNIVERSITY OF TECHNOLOGY
Department of Chemical Technology

Mari Aaltonen

THE DISSOLUTION KINETICS OF SPHALERITE CONCENTRATES

Thesis for the degree of Licentiate of Science in Technology.

Espoo 19.8.2005

Supervisor:
Kyösti Kontturi, Professor

Instructor:
Pekka Taskinen, PhD

Acknowledgements

The work for this thesis was conducted between March 2002 and May 2005 in the Laboratory of Physical Chemistry and Electrochemistry at the Helsinki University of Technology.

I want to thank Professor Kyösti Kontturi, the supervisor of this thesis, for his ideas and input throughout the process. I also wish to thank Pekka Taskinen, PhD., Olli Hyvärinen, PhD. and Marko Lahtinen, MSc. from Outokumpu Research Oy, for their instruction, advice and continuing interest, without which this work would not have been possible.

The help of the staff of the Laboratory of Physical Chemistry and Electrochemistry at HUT (many of whom I call friends – you know who you are :) is gratefully acknowledged and all the shared tea breaks warmly remembered. Thank you also to my friends outside the lab for providing plentiful relaxation amid all that hard work.

Most of all I want to thank my family: Mom, Dad, Kati and Jussi for always believing in me, no matter what my direction.

19th August, 2005

Mari Aaltonen

TEKNILLINEN KORKEAKOULU LISENSIAATINTYÖN TIIVISTELMÄ
Kemian tekniikan osasto

Tekijä Mari Aaltonen	Päiväys 19.8.2005
	Sivumäärä 70
Työn nimi Sphaleriittirikasteiden liukenemiskinetiikka	
Professuuri Fysikaalinen kemia	Koodi Kem-31
Työn valvoja Prof. Kyösti Kontturi	
Työn ohjaaja TkT Pekka Taskinen	

Työn kirjallisuusosassa annetaan yleiskuva sphaleriitin hapettavan liuotuksen mekanismeista ja kinetiikasta. Liukenemisen nopeuteen vaikuttavat tekijät sekä joitain tutkimuksessa käytettäviä menetelmiä esitellään lyhyesti.

Työn kokeellisessa osassa käytettiin useita tutkimusmenetelmiä. Suoraliuotuskokeissa, joissa käytettiin mangaanidioksidia sekä ferri-ioneita hapettajina, todettiin MnO_2:n vaikuttavan sphaleriittirikasteen liukenemiseen kahdella tavalla: se suoraan liuottaa sulfidimineraalia sekä regeneroi hapettavaa ferri-ionia. Tulokset myös viittaavat siihen, että mangaanidioksidi hapettaa partikkelien pinnalle muodostavaa elementääririkkikerrosta.

Kahden rikasteen liukenemiskinetiikkaa tutkittiin suoraliuotuskokeissa, joissa käytettiin ferrirautaa hapettimena rikkihappoliuoksissa. Rikasteet oli jaettu fraktioihin < 37 µm ja > 37 µm ja koeolosuhteet oli valittu vastaamaan teollista tuotantoa. Rikastefraktioiden keskimääriset sinkkikonversiot kolmen tunnin liuotuksen jälkeen olivat 45:stä 74:än massaprosenttiin. Rikasteen kokofraktio sekä liuoksen lämpötila ja ferrirautapitoisuus vaikuttivat voimakkaasti konversioihin. Hapon konsentraatiolla ja sinkkipitoisuudella ei ollut huomattavaa vaikutusta. Odotetusti konversio oli suurinta rikastefraktiolla, jolla oli suurin ominaispinta-ala ja konversiot laskivat pienenevän pinta-alan mukaisesti. Konversiot olivat keskimäärin 15 massaprosenttia korkeampia sillä rikasteella, jonka hilassa oli enemmän rautaa, kun keskimääräiset konversiot jaettiin rikasteiden ominaispinta-aloilla.

Tutkimusta varten tehtiin pyörivä rengas-levy-elektrodi, jossa käytettiin levyelektrodina rikasteesta puristettua nappia. Ferrorauta, jota syntyi kun ferrirauta hapetti rikastetta, detektoitiin platinaisella rengaselektrodilla hapettamalla se takaisin ferrimuotoon. Rengaselektrodin virran avulla määritettiin liuekenemisnopeus. Menetelmä on nopea ja sopii rikasteiden liukenemisominaisuuksien vertailuun eri olosuhteissa. Lisäksi menetelmän avulla saadaan erotettua aineensiirron ja kinetiikan vaikutukset, jolloin voidaan tarkemmin tutkia reaktiokinetiikkaan vaikuttavia tekijöitä. Teoreettiset aineensiirtolaskut osoittivat, että kinetiikka on reaktionopeutta rajoittava vaihe. Parantamalla aineensiirtoa liuoksessa ei voida nopeuttaa liukenemista, vaan olosuhteita tulee muuttaa kineettisten vaiheen nopeuttaiseksi.

Mineraali-hiilipastaelektrodi tehtiin sekoittamalla sphaleriittirikastetta hienon hiilijauheen ja öljyn kanssa. Mitatut sykliset voltamogrammit osoittavat, että hiili-öljypastaelektrodi oli inertti käytetyissä olosuhteissa. Modifioidulla mineraalielektrodilla tehdyillä voltametrisillä ja potentiostaattisilla mittauksilla tutkittiin potentiaalin vaikutusta liukenemisnopeuteen. Sulfidin liukeneminen alkoi 0,8 V:n (vs. Ag/AgCl) potentiaalissa ja reaktionopeus kasvoi potentiaalin noustessa 1,2 volttiin (vs. Ag/AgCl) saakka.

HELSINKI UNIVERSITY OF TECHNOLOGY ABSTRACT OF LICENTIATE THESIS
Department of Chemical Technology

Author Mari Aaltonen	Date 19.8.2005
	Pages 70
Title of thesis The Dissolution Kinetics of Sphalerite Concentrates	
Chair Physical Chemistry	Chair code Kem-31
Supervisor Kyösti Kontturi, Professor	
Instructor Pekka Taskinen, PhD	

In the literature part of the thesis, an overview of the mechanisms and kinetics of oxidative sphalerite dissolution was given. The factors affecting the rate of dissolution and some methods of study were briefly described.

In the experimental part various methods were used. In batch dissolution experiments with manganese dioxide and ferric ions as the oxidising species, it was found that MnO_2 affects the dissolution of a sphalerite concentrate by two mechanisms: by directly oxidising the sulphur in the mineral and by regenerating the active ferric species. The results also suggested further oxidation of the elemental sulphur layer by the manganese species.

The dissolution behaviour of two sphalerite concentrates was studied by batch dissolution experiments using ferric ions as the oxidant. Fractions with particle sizes of < 37 µm and > 37 µm were used. The measurement parameters were chosen to match those in industrial scale dissolution. The average zinc conversions for the fractions were from 45 to 74 mass percent after 3 hours dissolution. The conversions were strongly effected by the size fraction of the concentrate, temperature and the concentration of iron in the solution. The effects of the sulphuric acid and zinc concentrations were on average negligible. As expected, the concentrate fraction with the largest surface area per gram had the highest conversion and the conversions decreased with decreasing surface area. The average conversion divided by the surface area of the concentrate was 15 m-% higher for the concentrate with a higher concentration of iron in the lattice.

A rotating ring disc electrode was constructed, in which a pressed concentrate pellet was used as the disc. The Fe^{2+} ions formed by the dissolution of ZnS in the disc were detected on the platinum ring by oxidising them back to the ferric form. The measured current was used to determine the rate of dissolution. The method is fast and thus can be used for rapid comparison of the dissolution characteristics of different concentrate fractions under varying conditions. In addition, the method allows for the effects of kinetics and transport processes on the current to be separated, allowing a closer study of the factors affecting the kinetics of the reaction. Theoretical calculations of the rate of mass transfer showed, that kinetics are rate limiting under these conditions. Increasing the mass transport in the solution will not increase the rate of the dissolution process; the conditions have to be made more favourable for faster kinetics.

A mineral-carbon paste electrode was constructed by mixing sphalerite concentrate with fine carbon powder and oil. Cyclic voltammetric measurements showed the carbon-oil paste electrode to be inert under the conditions used. The voltammetric and potentiostatic measurements conducted on the modified mineral electrode showed the effect of the electrode potential on the rate of dissolution. The oxidation of the sulphide began above 0.8 V vs. Ag/AgCl and the rate was increased with increasing potential until a maximum was reached at 1.2 V vs. Ag/AgCl.

LIST OF SYMBOLS

A	pre-exponential factor (eq. 24)	
A	surface-area of the electrode (eq. 31)	[m^2]
A_0	total initial area available for reaction (eq. 13)	[m^2]
b	stoichiometric coefficient (eq. 6, 8, 9)	
c^b	bulk concentration of the reacting species	[mol/l]
c_{fs}	concentration of Fe^{3+} in the sulphur layer (eq. 6, 8, 9)	[mol/l]
D	diffusion coefficient of reacting species	[cm^2/min]
D_e	effective diffusion coefficient of ions in porous medium (eq. 8, 9)	[cm^2/min]
E	solution potential (eq.34)	[V]
E^0	standard electrode potential of the reaction	[V]
E_a	activation energy	[kJ/mol]
E_h	redox potential of the solution vs. Ag/AgCl (eq. 13)	[V]
F	Faraday constant	[C/mol]
I	total current	[A]
$I_{B\text{-}V}$	kinetic current	[A]
I_{diff}	diffusion current	[A]
I_0	equilibrium current	[A]
K	rate of dissolution (eq. 25)	[g g^{-1} m^{-2} h^{-1}]
k_c	rate constant of the reaction (eq. 24)	
k_c	rate constant of the surface reaction (eq. 5 and 6)	[min^{-1}]
k_{cc}	chemical rate constant (eq. 6, 9)	[cm/min]
k_d	rate constant for diffusion (eq. 7, 8)	[min^{-1}]
M	amount of leachable material remaining in particle cores (eq. 13)	[mol]
M_0	initial value of M (eq. 13)	[mol]
M	molecular weight of sulphide mineral (eq. 6, 8, 9)	[g/mol]
n	number of electrons in a unit reaction	
r	radius of the reacted particle (eq. 6, 8, 9)	[cm]

r_0	radius of the unreacted particle (eq. 6, 8, 9)	[cm]
R	molar gas constant	[J/(mol K)]
t	reaction time	[min]
T	absolute temperature	[K]
X	conversion	
α	transfer coefficient	
η	over potential	[V]
ρ_z	density of sulphide mineral (eq. 6, 8, 9)	[g/cm^3]
υ	kinematic viscosity	[m^2/s]
ω	angular speed of the electrode	[rad/s]
[i]	concentration of i	[mol/l]
[$\%\ Fe$]	iron content of the mineral (eq. 25)	[%]
P_i	partial pressure of i	[Pa]

Abbreviations

AAS	atomic absorbance spectroscopy

1. INTRODUCTION

Sphalerite is by far the most processed zinc mineral and annually over 7 million tonnes (2003) of zinc is produced by the treatment of sphalerite concentrates [1]. In the traditional roast-leach-electrolysis process the concentrate is combusted to a soluble oxide, dissolved into acid and the zinc is recovered by electrowinning. The roasting process also produces sulphur dioxide, which can no longer be released into the atmosphere due to ecological legislation. The sulphur dioxide has to be treated into a more storable form, and is usually processed into sulphuric acid. This is not economically viable, due to the over production of the acid and thus new production methods for zinc are of great interest.

The roasting step was first replaced by direct, oxidative leaching under high pressure and later, an atmospheric leaching process was taken to use [1]. Both of these methods oxidise the sulphur into elemental form so it can easily be collected and stored. These methods are often used alongside the roasting process and concentrates are divided between the processes by their characteristics. Some research is concentrating on the possibilities of a biological oxidation step to be incorporated with the direct leaching process [1].

Although the industrial processes have been in use for many years, there is still controversy on the kinetics and mechanisms of the dissolution reaction in direct oxidative leaching. This is partly due to the variety of concentrates used, as the amounts of impurities, especially iron, in the sulphide lattice have a strong effect on the dissolution rate. In addition, the effects of catalytic agents, surface-active agents, oxidative species, and mechanical activation, stirring rate and reaction time on their part explain the lack of a comprehensive model for this dissolution phenomenon.

2. LEACHING OF SPHALERITE

2.1 DIRECT OXIDATIVE LEACHING

Zinc can be released for processing from sphalerite concentrate by oxidative dissolution. A multitude of studies has been published using various solutions and oxidants [2, 3, 4, 5, 6].

Ferric sulphate is a common oxidising agent in sphalerite dissolution and the dissolution into hot sulphuric acid can be conducted at atmospheric pressure. The sulphur in the concentrate is oxidised to elemental form by the ferric ions, and as the lattice is broken down, the zinc is released into the solution according to equation 1 [7, 8, 9]:

$$ZnS\,(s) + 2\,Fe^{3+}\,(aq) \rightarrow Zn^{2+}\,(aq) + 2\,Fe^{2+}\,(aq) + S\,(s) \qquad (1)$$

If oxygen is present in the system, the ferrous ions can be oxidised to the ferric form according to reaction 2 [1, 9]:

$$2\,Fe^{2+}\,(aq) + H_2SO_4\,(aq) + ½\,O_2\,(g) \rightarrow 2\,Fe^{3+}\,(aq) + SO_4^{2-}\,(aq) + H_2O \qquad (2)$$

In both pressure and atmospheric leaching it has been noted, that direct oxidation of concentrate by oxygen is minimal [1]. The solution potential is determined by the ferric to ferrous ion ratio [2], so if there is no oxygen, or not enough of it, the potential of the solution decreases with reaction time. With an abundance of oxygen in the system, the total reaction becomes:

$$ZnS\,(aq) + H_2SO_4\,(aq) + ½\,O_2\,(g) \rightarrow ZnSO_4\,(aq) + S\,(s) + H_2O \qquad (3)$$

At temperatures below 150 °C elemental sulphur is the main sulphur product, only at higher temperatures in pressure leaching conditions, sulphates begin to form [1]. The elemental sulphur formed remains on the surface of the particle and the

reactive core of the particle shrinks during the dissolution according to the Shrinking core model [4, 8, 10, 11]. Layers of differing composition and stoichiometry are formed within the concentrate particle and the rate of diffusion of ferric ions to the ZnS lattice is reduced as the topmost layers are depleted in zinc. Likewise, the rate of diffusion of the products away from the reaction zone is reduced. These effects can be seen as a reduction on the over all reaction rate. If the oxidation potential in the solution is high enough, the elemental sulphur layer can be further oxidised into a soluble sulphate form according to reaction 4 [12]:

$$S\,(s) + 6\,Fe^{3+}\,(aq) + 4\,H_2O \rightarrow 8\,H^{+}\,(aq) + SO_4^{2-}\,(aq) + 6\,Fe^{2+}\,(aq) \qquad (4)$$

The dissolution reactions are electrochemical in nature and in the beginning of dissolution charge transfer at the surface is the rate-determining step. This mechanism explains why increase in the solid solution iron content or dissolved Ag, Hg and Bi (catalytic effect), increase the rate of dissolution. The effect of mechanical activation may also be explained. [1]

2.2 SELECTIVE EXTRACTION

In nature, zinc is often associated with other sulphides, such as iron sulphides (pyrite and pyrrhotite), copper sulphides (covellite), copper-iron sulphides (chalcopyrite) and lead sulphides (galena) [13,14]. These sulphides are difficult to separate by traditional separation techniques such as selective flotation. However, hydrometallurgical methods can be applied to selectively dissolve the metals, as the optimum leaching conditions of the minerals vary, as do the rates of dissolution.

The selectivity of the process can be increased by addition of roasting steps at different temperatures. Akcil and Ciftci [14] reported recoveries of 97 % for copper and 90 % for zinc in a combined thermal treatment – pressure leaching process for the mixed sulphide. The sulphide was roasted firstly at 400 °C and the

zinc was dissolved in a leaching step. The roasting was repeated at 620°C, after which the copper was dissolved and recovered.

A heterogenous mixture of sulphides has areas of varying potential and galvanic coupling is known to greatly affect the rates of dissolution [14, 15]. The sulphide with the higher rest potential becomes the cathode and supports the reduction of the oxidising agent; the one of lower potential becomes the anode and dissolves. The oxidation potential of sphalerite is lower than that of e.g. copper sulphide and dissolution of zinc by selective extraction is possible from a mixed zinc-copper sulphide [16]. Pyrite also is known to enhance the dissolution of sphalerite by galvanic coupling [14, 17].

Palencia *et al*. [16] studied the acidic ferric sulphate solution of a copper/zinc sulphide. They found that the galvanic interaction between the sphalerite and chalcopyrite resulted in the selective extraction of zinc. Zinc conversion of nearly 80 % was achieved, and after the separation of solid sulphur and lead sulphate from the residue, it could be used as a copper concentrate for a pyrometallurgical recovery process.

2.3 BIOLEACHING

The use of bacteria, such as *Thiobacillus ferroxidans,* in oxidative leaching has been studied for several years [5, 16, 18, 19]. There is disagreement on the role of different mechanisms of bioleaching. There are three proposed ways in which *T. ferroxidans* can participate in the dissolution reaction of minerals in ferric sulphate containing media [17, 18]. Firstly, in the direct oxidation of the mineral, the bacteria attack the mineral lattice oxidising the sulphur and freeing the metal into the solution. Secondly, the bacteria can oxidise the ferrous ions in the solution to ferric ions, which then attack the lattice. Thirdly, the bacteria can attack the sulphur layer, which forms in many mineral surfaces during dissolution and slows down the reaction rate. As the surface is kept clean, mass transport is not hindered and the reaction continues at a greater rate. The relative importance

of these mechanisms is disputed, but the oxidation of the ferrous ions to the ferric form seems to be of major importance [1]. However, the mechanisms may also be dependent on the experimental conditions.

Selvi *et al*. [5] studied the electrobioleaching of sphalerite with the *T. ferroxidans* at different potentials, as the electrobioleaching process produces current and thus an applied potential can affect the rate of reaction. They found the leaching at a positive potential (+0.4 V (SCE)) to be more efficient than that at the lower potential (-0.5 V (SCE)). They also concluded, that at the higher potential the direct attack mechanism becomes predominant and the elemental sulphur layer is oxidised by the bacteria.

Fowler *et al*. [18] likewise studied the dissolution of zinc sulphide and concluded that the reaction at the mineral surface was the rate-determining step at low ferrous ion concentrations. At higher ferrous ion concentrations, the diffusion of this species through the elemental sulphur layer would be the rate-determining step. They proposed, that the bacteria only affect the process by removing the elemental sulphur layer from the particle surfaces. Long *et al*. [19] studied the effects of ferrous ion concentration on the performance of a strain of immobilised *T. ferroxidans, A. ferroxidans,* and found high ferrous concentrations to reduce the activity of the immobilised bacteria.

3. MECHANISM AND KINETICS OF OXIDATIVE LEACHING

Many metals are processed from their sulphide ores and the behaviour of sulphur during the leaching processes is very important. In the minerals, the sulphur is in the –2 oxidation state and as it is oxidised to the elemental form, the metal ions are released into the solution. Intermediate polysulphide species, formed through covalent chains, have also been found. Elemental sulphur is quite stable in aqueous conditions, but can be further oxidised to the +6 state, thus forming sulphates SO_4^{2-}, by oxidising species or applied potentials [20, 21].

3.1 THE SHRINKING CORE MODEL

The shrinking core model describes dissolution processes, where one or more of the reaction products is insoluble and remains on the surface of the dissolving particle. The total radius of the particle remains constant throughout the process, while depleted layers of varying stoichiometries are formed inside the particle. The rate of dissolution can be governed by four different processes: 1) the mass transfer of reagents and products through the solution, between the particle surface and the bulk solution, 2) The diffusion of reagents and products through the product layer in the particle, between the surfaces of the particle and the reacting core, 3) a chemical reaction and 4) a charge transfer reaction.

In the beginning of the sphalerite concentrate dissolution the rate of reaction is determined by the electron transfer reaction at the surface of the particle. When the shrinking core model for spherical particles is obeyed, the rate of reaction is dependent on the conversion, X, according to equation 5: [4, 10]

$$k_c t = 1 - (1-X)^{1/3} \qquad (5)$$

where t is the reaction time, X is the conversion, given by $1 - (r/r_0)^3$ and k_c is the rate constant for the reaction, given by [4]:

$$k_c = \frac{Mbk_{cc}c_{fs}}{r_0\rho_z} \tag{6}$$

where M is the molecular weight of the sulphide mineral, b is the stoichiometric coefficient, k_{cc} is the chemical rate constant, c_{fs} is the concentration of Fe^{3+} in the sulphur layer on the mineral surface, r_0 is the radius of the unreacted particle, r is the radius of the reacted particle and ρ_z is the density of sulphide mineral.

As the process continues, the forming layer of elemental sulphur hinders diffusion slowing down the reaction until the diffusion through this layer becomes the rate-determining step. In this case the rate of reaction can be expressed by the Crank-Ginstling and Brounstein model for diffusion through a non-porous product layer [4, 10]:

$$k_d t = 1 - \frac{2}{3}X - (1-X)^{2/3} \tag{7}$$

where k_d is the rate constant for diffusion, given by [4]:

$$k_d = \frac{2MbD_e c_{fs}}{r_0^2\rho_z} \tag{8}$$

where D_e is the effective diffusion coefficient of ions in porous medium.

The conversion of the concentrate is dependent both on the mass transport in the system and the parameters affecting the kinetic rate of reaction, such as solution potential and temperature. Equations 5 and 7 apply only to the special cases when either the surface reaction or diffusion fully controls the rate of reaction. During most of the dissolution process a combination of the two equations is needed to express or predetermine the rate. If the two rates are of equal magnitude, their combined, mixed-kinetics equation becomes:

$$\frac{Mbk_{cc}D_e c_{fs}}{r_0^2 \rho_z} t = \frac{D_e}{r_0}\left[1-(1-X)^{1/3}\right] + \frac{k_{cc}}{2}\left[1-\frac{2}{3}X-(1-X)^{2/3}\right] \quad (9)$$

Dutrixac *et al*. [1] studied the conditions under which the shrinking core model is applicable for the dissolution of sphalerite. They found, that the model is obeyed when the rate of roughening of the surface and the decrease in free mineral surface area due to the sulphur layer and agglomeration are equal. This is because the model assumes the surface area of the particle to remain uniform throughout the measurement, and only the surface area of the reactive mineral surface to reduce with time.

The effects of product mass transfer through a liquid film and diffusion control caused by product solubility limitations could be studied by an extension to the shrinking core model proposed by Lapidus *et al*. [22]. This complex kinetic equation was applied to experimental data on the ammoniacal leaching of zinc with cupric chloride and the results support the theory of product diffusion control.

3.2 FERRIC SULPHATE AS AN OXIDANT

3.2.1 Pressure leaching

The kinetics and mechanisms of the pressure leaching of sphalerite have been under study for decades. The dissolution takes place through formation of H_2S, according to reactions 10-12 [23, 24, 25]:

$$ZnS + H_2SO_4 \rightarrow ZnSO_4 + H_2S \quad (10)$$

$$H_2S + Fe_2(SO_4)_3 \rightarrow 2\ FeSO_4 + S + H_2SO_4 \quad (11)$$

$$2\ FeSO_4 + H_2SO_4 + ½O_2 \rightarrow Fe_2(SO_4)_3 + H_2O \quad (12)$$

Jan *et al.* [23] showed, that the heterogeneous oxidation of hydrogen sulphide to elemental sulphur at the sphalerite surface was rate controlling, instead of the homogenous reaction in the solution. They also stated, that the mineral was oxidised by the ferric ions in the solution, not by direct oxidation by oxygen. The role of the oxygen was to re-oxidise the ferrous ions to the ferric form. Currently, this has been accepted by most other researchers.

Verbaan and Crundwell [2] derived a model for the dissolution of sphalerite in sulphuric acid with ferric sulphate as the oxidant in pressure leaching conditions. It is a charge-transfer model, in which the potential of the mineral surface is approximated by the solution redox potential for the Fe^{2+}/Fe^{3+} redox couple. The rate of the dissolution is expressed by equation 13:

$$-\frac{dM}{dt} = 6.505\frac{mol}{l \cdot s}\exp(\frac{-79.4J/mol}{RT})\frac{A_0}{m^2}(M/M_0)^{2/3}\exp(\frac{17.3}{V}E_h) \qquad (13)$$

where M is the amount of leachable material remaining in particle cores, M_0 is the initial value of M, A_0 is the total initial area available for reaction and E_h is the redox potential of the solution vs. Ag/AgCl.

The rate of ferrous-ion oxidation was expressed by (14):

$$\frac{d[Fe(III)]}{dt} = 2.08 \cdot 10^9 \frac{l^{1.65}}{mol^{1.65} \cdot s}\frac{[Fe(II)]^2[O_2]}{[H^+]^{0.35}}\exp(\frac{-68.6J/mol}{RT}) \qquad (14)$$

where $[Fe(III)]$ is the concentration of Fe^{3+}, $[Fe(II)]$ is the concentration of Fe^{2+}, $[O_2]$ is the concentration of O_2 and $[H^+]$ is the concentration of H^+. The simultaneous integration of equations 10 and 11 results in an expression, which well predicted experimental results.

Courriou *et al.* [24] studied the thermodynamics and kinetics of synthetic ZnS dissolution in sulphuric acid under pressure leaching conditions with and without

oxygen present. They corroborated earlier studies [23] and found the rate of reaction in the presence of oxygen to be chemically controlled by the oxidation of hydrogen sulphide. They found the concentration of dissolved zinc to be dependent on the surface area of the ZnS, the initial partial pressure of oxygen and the initial sulphuric acid concentration.

The oxidation of the ferrous ions formed during ferric oxidative pressure leaching of sphalerite was studied by Dresinger *et al.* [25]. They postulated, that the free ferrous ions are less easily oxidised than the ion pair $FeSO_4$, and formed an empirical equation for the rate of ferrous oxidation:

$$\frac{-d[Fe^{2+}]}{dt} = (3.6\times10^{-5}[Fe^{2+}]^2 P_{O_2} + 5.2\times10^{-4}[Fe^{2+}][FeSO_4]P_{O_2} + 1.66\times10^{-2} \times [FeSO_4]^2 P_{O_2}) \times (1.0 + 5.0[CuSO_4]^{0.5}) \left\{ \exp\left[-9660\left(\frac{1}{T} - \frac{1}{423.15} \right) \right] \right\}, \quad (15)$$

where $[Fe^{2+}]$ is the concentration of Fe^{2+}, $[FeSO_4]$ is the concentration of $FeSO_4$, $[CuSO_4]$ is the concentration of $CuSO_4$, P_{O2} is the partial pressure of oxygen and T is the reaction temperature in Kelvin.

These empirical kinetic expressions are far from a comprehensive model for the leaching process, but do further the understanding of the reactions involved. Likewise, the results from pressure leaching experiments cannot be directly applied to atmospheric leaching, but give a good basis to build upon.

3.2.2 Atmospheric leaching

Dutrizac *et al*. [1] made surface studies of fracture exposed sphalerite surfaces at different stages of dissolution in ferric sulphate - sulphuric acid media to determine a more detailed reaction sequence than portrayed by equations 1 and 2. They concluded, that firstly, a region a few atomic layers thick is leached of zinc

forming a polysulphide of variable composition, which could be described as a dynamic metal-deficient sulphide:

$$(1+y)\ ZnS + 2y\ Fe^{3+} \rightarrow y\ Zn^{2+} + ZnS_{1+y} + 2y\ Fe^{2+} \quad (16)$$

The oxidation continues until a distinct polysulphide phase with a defined composition is formed:

$$(1+x)\ ZnS + 2x\ Fe^{3+} \rightarrow x\ Zn^{2+} + ZnS_{1+x} + 2x\ Fe^{2+}, \quad x>y \quad (17)$$

This phase then reacts to form elemental sulphur:

$$ZnS_{1+x} + (2+2x)\ Fe^{3+} \rightarrow Zn^{2+} + (2+2x)\ Fe^{2+} + (1+x)\ S^0 \quad (18)$$

This causes a uniform sulphur layer to form on the surface. It seems another mechanism for the sulphur formation is needed to explain the formation of isolated sulphur globules. A deposition from solution would explain the formation of euhedral sulphur crystals at the active sites on the surface, such as grain boundaries and other surface defects. The proposed mechanism is [1]:

$$ZnS_{1+x} + 2H^+ \rightarrow Zn^{2+} + H_2S\ (aq) \quad (19)$$

$$H_2S\ (aq) \rightarrow HS^- + H^+ \quad (20)$$

$$HS^- + 2\ Fe^{3+} \rightarrow S^0 + 2\ Fe^{2+} + H^+ \quad (21)$$

This dissolution – deposition route would result in the observed isolated sulphur globules and euhedral sulphur crystals.

3.3 MANGANESE DIOXIDE AS AN OXIDANT

Minerals are known to participate in galvanic interactions with each other as well as with metals [26, 27, 28]. Sphalerite can be oxidised by contact with manganese

dioxide, a process in which both dissolve. The Mn(IV)-oxide is stable in aqueous solutions, but can be electrochemically reduced to the valence +2. This is the most stable state of manganese in aqueous solutions and in acidic solutions it is present as the Mn^{2+} ion [29]. The reaction takes place through galvanic interactions between the solids and is described by equation 22 [27, 28]:

$$ZnS + MnO_2 + 4\ H^+ \rightarrow Zn^{2+} + Mn^{2+} + S^0 + 2\ H_2O \qquad (22)$$

Madhuchhanda *et al*. [27] studied the interactions between MnO_2 and sulphide minerals using leaching studies and polarisation measurements. The polarisation measurements gave information on the galvanic effect between the minerals. In the case of a sphalerite electrode coupled to a MnO_2 electrode, the reaction rate was found to be under mixed control of the cathodic reduction of MnO_2 and the diffusion controlled oxidation of the sphalerite anode. The leaching experiments gave information on the rate of reaction in a suspension of the two solids in an acid medium. The amount of solids is of absolute importance, since now the galvanic connections take place only when the particles collide in the solution. It was shown that the zinc dissolution current increased from 0.24 mA/cm^2, with 2 g of sphalerite and 4 g of MnO_2 to 0.36 mA/cm^2 with 10 grams of both solids in 100 ml of sulphuric acid.

When ferrous ions are also present in the solution, a reaction between the ferrous ions and manganese dioxide may occur according to equation 23:

$$2\ Fe^{2+} + MnO_2 + 4\ H^+ \rightarrow 2\ Fe^{3+} + Mn^{2+} + 2\ H_2O \qquad (23)$$

These reactions shall be studied in more detail in the experimental part of this work. These reactions were also studied by Srinivasa *et al*. [28], who concluded from leaching experiments, that when ferric ions are present, they are the main species oxidising the sulphide lattice. The manganese dioxide participated in the process mainly by re-oxidising the ferrous ions formed.

4. FACTORS AFFECTING THE RATE OF DISSOLUTION

4.1 TEMPERATURE

As in most processes, temperature has a clear effect on the rate of sphalerite dissolution. The magnitude of the effect is given by the activation energy of the reaction E_a and the relation between temperature and the rate of reaction is given by the Arrhenius equation [30]:

$$k_c = Ae^{(-E_a/RT)} \tag{24}$$

where k_c is the rate constant of the reaction, A is the pre-exponential factor, E_a is the activation energy, R is the molar gas constant and T is the absolute temperature.

Diffusion is moderately dependent on temperature and the reported values for the activation energy of diffusion through a liquid range from 4.2-12.6 kJ/mol [4] to 20-25 kJ/mol [3]. When diffusion takes place through a porous layer, the E_a values are higher than in solution and are in the same range as for chemically controlled reactions. Chemical reactions are usually more dependent on the temperature and have reported activation energies greater than 42 kJ/mol [4] or 30 kJ/mol [3].

The activation energy values reported in literature for sulphide dissolution reactions vary somewhat. Weisener *et al.*. [3] calculated an E_a of 34 kJ/mol for the sphalerite dissolution reaction in perchloric acid with oxygen, while Bobek *et al.* [4] calculated an overall activation energy of 46.9 kJ/mol for the acidic ferric chloride leaching. It cannot be determined, whether the processes are under chemical control or controlled by diffusion through a porous layer, as the activation energy values for these processes lie in the same value range. Verbaan *et al*. [2] reported E_a values as high as 79.4 kJ/mol for the ferric sulphate dissolution of sphalerite in sulphuric acid. One reason for the differences in the values is the varying iron content of the sphalerites used. Crundwell *et al*. [8]

found the activation energies to change from 59 kJ/mol for a sphalerite with 0.5 % iron, to 32 kJ/mol for the mineral with 9.7 % iron.

The activation energy for the acid ferric sulphide dissolution of chalcopyrite was studied by Munoz *et al*. [31]. The chalcopyrite dissolves similarly to sphalerite, with an elemental sulphur layer forming on the particles. The electron conductivity of the product sulphur layer seemed to be the rate-limiting step, with an E_a of 83.7 kJ/mol. This corresponds nicely to the activation energy for electron conductivity measured in elemental sulphur, 96.3 kJ/mol.

4.2 PARTICLE SIZE AND MIXING

The particle size distribution of the sphalerite has a strong effect on the rate of dissolution [4, 9]. Bobeck *et al*. [4] found decreasing particle size and increasing surface area to enhance sphalerite dissolution, as is to be expected. This is naturally corroborated by other authors [23, 32]. Jan *et al*. [23] analysed the effect of particle size (44μm – 125 μm) on the pressure leaching of sphalerite with oxygen. The rate of dissolution was increased with surface area, which showed that the rate of oxygen dispersion was not the rate-determining step. If had been, particle size would not have affected the reaction rate.

The effect of agitation on the rate of dissolution has been studied in a multitude of papers, with largely varying conclusions [7, 16, 32]. Agitation affects the thickness of the diffusion layer surrounding the dissolving particles. The effect of the rate of agitation on the dissolution rate depends on the rate-determining step of the process. At low rates of agitation, diffusion in the diffusion layer can be the rate-determining step, and thus mixing does affect the rate of reaction. The rate of reaction increases with increasing agitation until diffusion in the solution is no longer rate determining. Above this level, the rate of agitation is non-consequential [4, 23]. The effects of particle size and agitation have to be considered together, since as the particle size is reduced, diffusion to the surface is enhanced and the effect of stirring becomes less pronounced.

The effects of agitation and particle size were more thoroughly analysed for the dissolution kinetics of human enamel powder [33, 34, 35]. As in sphalerite dissolution, a by-product layer is formed on the surfaces of the enamel particles and reduces the rate of dissolution. Gramain *et al*. [33] found the rate of dissolution at high stirring to be limited by diffusion through this by-product layer and at low stirring by diffusion in the Nernst layer adjacent to the surface deposited layer. A rigorous mathematical treatment of the high-stirring case was done by Hsu *et al*. [34, 35] and an explicit expression for the temporal variation in the size of the particles was obtained as well as an analytical expression for the effect of the particle size on the dissolution time.

4.3 COMPOSITION OF THE MINERAL

4.3.1 Iron content of the sphalerite

The dissolution of sphalerite is an electrochemical process, governed by the charge transfer at the surface. Thus it is natural, that the solid solution iron content of the sphalerite has a strong effect on the leaching rate as they have an effect on the number of occupied sites in the d-orbital conduction band of the (Z, Fe)S [11, 36].

Dutrizac *et al.* [1] studied the dissolution behaviour of five fracture-exposed sphalerite surfaces with iron contents from 0 % to 15 % in weight. The surface layers of the samples were analysed after dissolution with X-ray photoelectron spectroscopy, to give information of the changes in composition. The minerals with 8 and 15 % iron on the lattice reacted very rapidly from the very beginning of dissolution, while the ones of low iron content (<0.2 %) were quite non-reactive under the applied conditions.

Bobek *et al.* [4] compared the rate of dissolution for a pure ZnS powder and a mineral concentrate. They found the rate of dissolution to be considerably faster for the mineral concentrate. It was proposed, that the effect was due to the

presence of iron (5 %) in the sphalerite mineral. Impurities are believed to enhance the ionic character of the mineral, thus inducing faster dissolution.

A linear relation between spahlerite iron content and dissolution rate was found by Pelencia Perez *et al*. [11]. They studied fifteen sphalerite samples with 0.04 to14.7 % of iron in the mineral and found the data to yield an equation for the rate of reaction:

$$K\ (\mathrm{g\ g^{-1}\ m^{-2}\ h^{-1}}) = 0.219 + 0.258\ [\%\ \mathrm{Fe}] \qquad (25)$$

Their results suggested that the activation energy for the dissolution varied with the iron content of the mineral, with values ranging from 41 to 72 kJ/mol with decreasing iron content from 12.5 to 0.04 wt.%. Weisener [37] *et al*. found similar results for sphalerite dissolution in $HClO_4$. They measured activation energies of 63, 50 and 39 kJ/mol for samples with 0.45, 11.40 and 12.90 wt.% of iron. Halavaara [32] noted a similar increase in the rate of reaction as a function of iron content of the mineral, and found the rate-enhancing effect to cease, as diffusion through the product layer became rate determining.

Crundwell [36] studied the dissolution of sulphide minerals applying the fundamentals of semiconductor electrochemistry. He concluded, that mineral dissolution mostly takes place though a hole mechanism. He explained the effect of lattice iron on the rate of dissolution by the d-band energy levels within the band gap provided by the substitutional iron. This allows for easier transfer of electrons and pins the Fermi level at a level within the d-orbital band.

Kemmel *et al.* [38] measured the equilibrium potentials of sphalerite samples with varying iron content and found the relation to be linear. The sphalerite with the least iron (0.1 %) had a potential of over 600 mV vs. SHE, while the one with the highest iron content (10.3 %) had a potential below 300 mV vs. SHE. The other samples fit nicely on the adjoining line.

4.3.2 Other impurities in the mineral

Also other impurities in the ZnS lattice can have a crucial effect of the dissolution characteristics of the mineral. Crundwell [39] studied two sphalerite minerals, which could not be leached beyond 50 % conversion of zinc. The conversions were dependent on the particle size, which would suggest a rate-determining surface reaction. The minerals had a high lead content (2 %) and it was proposed that a layer of $PbSO_4$ or lead jarosite was formed on the surface hindering dissolution. These lead species are insoluble in sulphate solutions, but dissolve in chloride solutions. No passivation of the sphalerite surfaces was found in chloride solutions, which supports the theory of insoluble lead species formation.

Buckley *et al*. [40] studied the surface compositions of two sphalerite samples under leaching conditions with oxygen or nitric acid as the oxidant. They found, that when zinc is leached into the solution and a metal-deficient sulphide is formed, copper in the lattice diffuses from the bulk mineral to the vacant cation sites near the surface. They proposed, that it was this copper-enriched layer, not the elemental sulphur layer, which hindered the dissolution process.

4.4 MECHANICAL ACTIVATION AND LATTICE DEFORMATIONS

Kammel *et al*. [38] reported an increase in zinc extraction from 68% to above 95% by grinding sphalerite to smaller particle size before leaching with sulphuric acid. They found, that 10 minutes of grinding in a semi-industrial attritor was sufficient, further grinding no longer increased the conversions. Energy on 20 kWh per tonne of sphalerite concentrate was enough to increase the conversion of zinc up to 91 %.

Balaz *et al*. [41] studied how mechanical activation by grinding affects the rate of sphalerite dissolution in hydrogen peroxide. Under the same conditions, the activation of the concentrate increased zinc conversion from 17 % to 65 –100 %. They also noted, that a maximum in surface area is reached, after which the

increase in surface area is counterbalanced by the formation of agglomerates. A XRD-study showed, that the grinding results in the decrease of crystalline phase of the mineral; the increase in lattice defects is seen as increasing amorphisation. In a further study [42] on the mechanochemistry of sulphide minerals they found, that the leaching rates of both zinc and iron are increased by the mechanical activation of a high-iron concentrate. They also found, that the selectivity of leaching was directly influenced by the surface disorder of the sphalerite.

Xiao *et al*. [43] used a thermochemical cycle to measure the mechanically activated storage energy of minerals, the excess energy stored in the lattices as dislocations and structural defects as a result of mechanical treatment. The energy was found to increase with activation time and was independent of the total surface-area.

Mikhlin *et al.* [44] explained the leaching behaviour of minerals by the formation and transformations of non-equilibrium metal-depleted layers (NL), with sulphur centers acting as dopants. The electrochemical properties of the mineral surface are determined by this layer, which causes the semi-conducting properties of the NL to become non-uniform. Thus, the NL should be considered a disordered semiconductor, with properties governed by negative correlation energy centres associated with sulphur atoms. The conductivity in a disordered semiconductor is low as movement of charge carriers is limited by being trapped in localised states and any heterogeneity has a significant effect on the properties of the semiconducting surface.

Naturally, the increased surface area reached by grinding increases the rate of the overall dissolution reaction. However, an understanding of the electrochemical mechanism of the dissolution is needed to see the other equally important effects of mechanical activation [1]. The grinding causes an increase in the number of lattice defects in the mineral surface, which can affect both the conductivity and stability of the crystals. Electrical conductivity is an essential factor in determining the rate of sulphide dissolution, as is the diffusion coefficient of the

metal ion in the sulphide lattice [45]. In addition, the activation energy of dissolution is decreased by mechanical activation, as bonds are broken in the crystalline lattice [42].

4.5 SOLUTION PARAMETERS

The species present in the solution effect the rate of dissolution, as is to be expected. High concentrations of the products naturally decrease the rate of reactions, as was found by Aaltonen [46] for the case of dissolved zinc in the leaching of sphalerite concentrates. Crundwell [8] explained the rate decreasing effect of Fe^{2+} ions by an indirect mechanism, in which the Fe^{2+} ions affect the concentrations of the oxidative species, Fe^{3+} and $FeHSO_4^{2+}$, in the solution.

Another important solution parameter is the pH, which can affect the rate of concentrate dissolution [7] as well as other reactions in the solution. For example, the feed of the oxidative leaching process contains iron in the form of jarosite, which is partially dissolved in the first stages of the leaching. In later stages of the dissolution, the concentration of sulphuric acid decreases and the pH rises, causing the precipitation of jarosite according to equation (26)[9]:

$$1½\ Fe_2(SO_4)_3 + ½\ (NH_4)_2SO_4 + 6\ H_2O \rightarrow NH_4Fe_3(SO_4)_2(OH)_6 + 3\ H_2SO_4 \qquad (26)$$

Other cations in the solution, such as K^+, Na^+, Pb^{2+} or H_3O^+, can also precipitate as jarosite.

4.6 CATALYSIS

Several species in the solution can catalyse the dissolution of sphalerite. Ferric ions were first considered as a catalytic species in the process [7], whereas now they are considered the actual oxidant. Also manganese dioxide has been listed as a catalyst [47] although it can perform as the oxidant [27]. These species have

been discussed in earlier sections. Other species can affect the leaching process, without directly participating in the lattice oxidation reaction. These are often present in small amounts.

The catalysts can affect process by various mechanisms. Cu^{2+} and Co^{2+} ions are known to have a catalytic effect on the air oxidation of ferrous ions, thus regenerating the active oxidising species [47]. Some species, such as Ag, Bi and Hg affect the surface layers of the mineral and cause changes in the electrochemical properties, for example increasing the conductivity of the layers [1]. Haung *et al*. [7] studied the catalytic effect of copper in the ZnS dissolution process. They found zinc ions in the lattice to be substituted by copper ions in the solution, which increases the conductivity of the surface layer thus enhancing dissolution. However, copper seemed to induce agglomeration of the concentrate, which hinders the reaction by reducing the total surface area. Buckley *et al*. [40] found copper from the bulk mineral to diffuse to the cation-depleted layer formed by zinc dissolution. In their leaching experiments with oxygen or nitric acid as the oxidant, this copper-enriched layer seemed to hinder the dissolution process. The addition of ferric ions into the solution removed the copper from the surface of the mineral and allowed dissolution to continue through the metal-deficient sulphide, which contained zinc as the only cationic species.

The catalytic effect of copper on the ferrous ion oxidation has been widely studied and seems to take place by reaction (27)[25, 47]:

$$Cu^{2+} + Fe^{2+} \rightarrow Cu^{+} + Fe^{3+} \qquad (27)$$

In acidic media, the Cu^{+} species can be oxidised by oxygen:

$$4\ Cu^{+} + O_2 + 4\ H^{+} \rightarrow 4\ Cu^{2+} + 2\ H_2O \qquad (28)$$

The Cu^{+} oxidation is faster than the direct oxidation of the ferrous species and thus copper addition increases the total rate of the dissolution reaction. An

analogous regeneration of the sphalerite oxidising species by cupric ions was presented by Ghosh *et al*. [48] for the case of the oxidative ammonia leaching of sphalerite.

Kemmel *et al.* [38] studied the effect of copper in the solution on the dissolution of zinc from sphalerite concentrates. They found the catalytic effect of Cu^{2+} to be dependent on the iron content of the mineral: for minerals with less than 1 % iron in the lattice, Zn extraction was enhanced by an addition of Cu^{2+} in the solution, while the extraction rate of minerals with a higher iron content was reduced by the copper addition. This phenomenon was explained by the formation of copper sulphide species. Potentiodynamic experiments on sphalerite electrodes showed CuS to be formed on the surfaces of a low iron-content mineral, while Cu_2S is formed on minerals with a high content of iron.

4.7 SURFACTANTS

The elemental sulphur forming on the concentrate particles seems to hinder the diffusion of reactants and products and lower the reaction rate. In conditions of pressure leaching, at temperatures over 119 °C, the sulphur melts and forms a compact layer on the surface, stopping the reaction [32]. Surface-active species are used to eliminate this effect.

Owusu *at al.* [6] studied the effects of three surfactants on the rate of sphalerite dissolution in pressure leaching conditions at elevated temperatures. The orthophenylene diamine (ODP), lignin sulphonic acid and metaphenylene diamine (MPD) dispersed the liquid sulphur and increased conversion from 50% in 1 hour to > 99%, 86-94% and 95-98% respectively. These results are comparable to the experiences of lignin sulphonic acid use in industry. Lignosulphonate was also studied by Lochmann *et al*. [10], who found that the use of 1 g/l lignosulfonate increased the conversion of zinc from 30% to 60% by coagulating the sulphur, forming a porous, penetrable matrix.

Haung *et al*. [7] used Quebracho, a tannic acid extract, in their sphalerite dissolution experiments and found it effective in removing elemental sulphur from the mineral surfaces. In large quantities, however, it seemed to decrease the rate of reaction.

In atmospheric dissolution processes, the elemental sulphur layer first grows in separated islands, which eventually join to form a uniform layer on the particle surface. This layer is not as compact as is formed by molten sulphur, but still has to be taken into consideration in the process. Elemental sulphur is very hydrofobic, causing the reacted particles to rise to the surface of the solutions. Surface-active species are used to disperse the particles into the solution for better dissolution as well as solution uniformity. A new method for the speciation and quantification of elemental sulphur on mineral surfaces was presented by Toniazzo *et al*. [49]. They combined the use of gas chromatography and mass spectrometry and studied the sulphur species forming on a pyrite surface. They found two different types of S_8 to form on the surface and believed this to be due to defects and impurities in the lattice.

5. METHODS FOR THE STUDY OF MINERALS AND CONCENTRATES

5.1 ROTATING RING DISC ELECTRODE

The rotating ring disc electrode is a useful tool for separating the effects of kinetics and mass transport when studying electrochemical phenomena. The rotating motion causes a steady flux of solution to the electrode surface and the thickness of the stagnant diffusion layer can be controlled by the rotation speed. Species formed on the disc electrode can be detected at the ring by applying a suitable potential. Only a fraction of the species produced on the disc is detected on the ring. The collector efficiency is dependent on the geometry of the ring-disc electrode. The current on the disc electrode is formed according to equation (29):

$$\frac{1}{I} = \frac{1}{I_{B-V}} + \frac{1}{I_{diff}} \tag{29}$$

where I is the total current, $I_{B\text{-}V}$ is the kinetic current according to the Butler-Volmer equation (30) and I_{diff} the diffusion current according to the Levich equation (31) :

$$I_{B-V} = I_0\left[\exp\left((1-\alpha)f\eta\right) - \exp(-\alpha f\eta)\right] \tag{30}$$

where I_0 is the equilibrium current, a the transfer coefficient, f=nF/(RT) and η the over potential.

$$I = 0.620nFAD^{2/3}\upsilon^{-1/6}\omega^{1/2}c^b \tag{31}$$

where D is the diffusion coefficient of the reacting species, υ the kinematic viscosity (viscosity divided by the density) of the solution, ω the angular speed of the electrode and c^b the bulk concentration of the reacting species.

When the rotation speed is increased, the diffusion layer becomes thinner and diffusion to the electrode is faster; at infinite rotation speed the current is fully dominated by the reaction at the electrode surface. Thus, the kinetic current can be obtained by extrapolation from a graph expressing $1/I$ as a function of $\omega^{-½}$.

Ring-disc electrodes have been used for the study of conductive minerals, such as pyrite [50], usually using electrodes fractured directly from the rock. A method using concentrate pellets is presented in the experimental section of this study.

5.2 CARBON PASTE ELECTRODE

The specific electrical resistance of sphalerite is $6 \cdot 10^9$ ohm·cm at 90°C [23]; most other metal sulphides have values ten orders of magnitude lower. This causes a problem for the electrochemical study of sphalerite, as an electrode material has to have sufficient conductivity. Mixing the mineral with copper and iron into a sulphide matte or with graphite into a paste increases the conductance and allows the mixtures to be used as electrodes [51].

Srinivasan *et al*. [12, 52] studied the optimum composition for a mineral-carbon paste, with different proportions of concentrate, graphite and pitch. The best results were reached with conducting compact electrodes made from sphalerite and graphite by pressure and heat treatments. In their cyclic voltammetric measurements, the oxidation of the sulphide is clearly seen, as is the consequent oxidation of elemental sulphur to sulphate ions. On the reverse scan, the formation of elemental sulphur and possibly of H_2S is seen. Acid concentration and scan rate were found to increase the dissolution current.

Pesonen [53] analysed the dissolution of sulphide minerals with anodic polarisation, cyclic voltammetry and potentiostatic dissolution. A mineral-graphite paste electrode was used and found to be practically inert during the electrochemical measurements. An increase in the rate of mineral dissolution due to increased temperatures and suitable potentials was seen. Ahlberg *et al*. [54]

used a similar electrode; sphalerite with carbon paste and an organic binder, as a rotating disc electrode. They found the rate determining process in sphalerite dissolution to change with the potential as well as solution composition. Both of these studies showed the carbon paste to be inert during electrochemical measurements. Crundwell [8] however had found the contrary: the presence of graphite did affect the mechanism of sphalerite dissolution.

Zhang *et al.* [55] prepared a sphalerite-carbon paste electrode with carbon for better conductance and paraffin oil for homogeneity. They studied the electrochemistry of these electrodes in $HCl/FeCl_3$ solutions. From a cyclic voltammogram they could clearly define peaks for the oxidation of the sulphide to elemental sulphur, the oxidation of chloride anions to adsorbed chlorine gas, the oxygen formation reaction, the reduction of chlorine gas back to chloride ions, the reduction of elemental sulphur to sulphide ions and the hydrogen forming reaction. The addition of ferric chloride to the system changes the voltammogram, as the reduction and oxidation of the iron species become dominant. The other peaks disappeared or were deformed and displaced at $FeCl_3$ concentration of 0.02 mol/dm^3. Choi *et al.* [56] identified the same reactions in their own voltammograms with carbon paste electrodes in the same solutions. In addition, increases in dissolution current with increasing temperature and decrease in current due to zinc depletion with time were shown.

Nava *et al.* [57] used mineral-carbon paste electrodes to study the dissolution reactions of mixed sulphides. A concentrate with sphalerite (ZnS-63.4%), pyrite (FeS_2-20.1%), chalcopyrite ($CuFeS_2$-5%), galena (PbS-0.33%), tetrahedryte ($Cu_{12}Sb_4S_{13}$-0.45%) and arsenopyrite (FeAsS-0.4%) was made into an electrode and anodic potential pulses were applied. The sphalerite and galena were dissolved throughout the potential range 0-600 mV vs. SSE. The other minerals had multi-step dissolution mechanisms and the potential areas for the transformations could be found from the voltammograms. This can be of use in the processing of complex sulphide concentrates.

5.3 SURFACE STUDIES

A multitude of surface methods can be applied to the study of the dissolution phenomenon. Dutrizac *et al*. [1] used X-ray photoelectron spectroscopy (XPS) to study fracture-exposed surfaces of sphalerite samples before and after dissolution to find chemical state information on the first few nanometers of the surface. The high resolution S2p, Zn2p and Fe2p spectra showed that S is the active species in dissolution, with only negligible changes in Zn and Fe chemistry. The elemental ratios also suggested, that less than 5 % of the sulphur oxidised further to sulphate under these conditions. (100°C, 0.3 M $Fe(SO_4)_{1.5}$ – 0.3 M H_2SO_4). The dissolution process was shown to take place through the formation of polysulphide species and the formation of elemental sulphur on the mineral surface was seen as the reaction advances.

Waisener *et al*.[3] coupled XPS with time of flight secondary ion mass spectrometry (ToF-SIMS) to study the dissolution kinetics of sphalerite in perchloric acid and the formation of a polymeric sulphur species on the particles. The advantage of this combination is that the ToF-SIMS gives information on the first few monolayers of the surface, while the XPS is used to study the near-surface regimes. They concluded, that the sulphur layer does not hinder the kinetics of the dissolution reaction under the used conditions.

Fowler and Crundwell [18] used scanning electron microscopy (SEM) to confirm the attachment of bacteria on sphalerite surfaces and energy dispersive X-Ray microanalysis (EDAX) to show, that the surfaces with bacteria had no elemental sulphur layer unlike the ones untreated with bacterial solution. Mikhlin *et al*. [58] applied XPS, X-ray emission and absorption spectroscopies and Mössbauer spectroscopy to study the surface changes during chalcopyrite leaching. Chernyshova [59] used FTIR spectroelectrochemical measurements to show that the oxidation of galena and pyrite surfaces takes place through the formation of thiosulphate and polythionate species from the elemental sulphur layer on the particle surfaces. Laser-induced oxidation of galena to oxysulphates was studied

by Shapter *et al*. [60] using Raman spectroscopy and the method was found applicable for the easy identification of galena in complex ores. Kendelewicz *et al*. [61] used photoemission spectroscopy to show that elemental sulphur and sulphur oxoanions were intermediate products in the oxidation of pyrite surfaces with molecular oxygen.

These surface methods, coupled with batch dissolution experiments and electrochemical analysis techniques, help to build a better understanding of the mechanism and kinetics of mineral dissolution behaviour. They allow for the detection of surface changes in the very beginning of the process and give information on the formation of intermediate species.

EXPERIMENTAL

6 DISSOLUTION EXPERIMENTS WITH MANGANESE DIOXIDE

A study of sphalerite dissolution with ferric ions as the oxidant was conducted and is reported in reference [46]. Batch dissolution experiments were conducted to study the applicability of manganese dioxide as the oxidant and the results were compared to those of the earlier study. The possible reactions between manganese dioxide and ferrous ions and elemental sulphur were investigated.

6.1 MATERIALS

Concentrate A, a sphalerite concentrate of 54 – 105 μm diameter was used in all experiments and its composition is given in Figure 1. Sulphuric acid solution (0.2 M) was diluted from concentrated H_2SO_4 (Merck) with MilliPore ion-exchanged distilled water. Manganese dioxide (Merck) and ferric and ferrous sulphates (Riedel-de Haën) were of reagent grade.

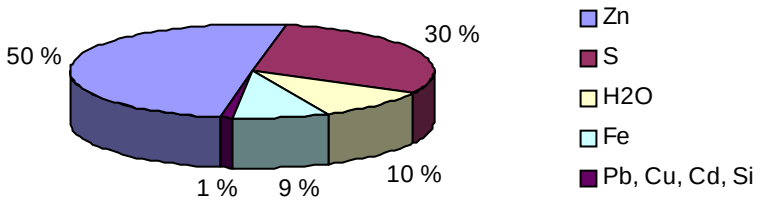

Figure 1. The composition of Concentrate A.

6.2 EQUIPMENT

The dissolution experiments were conducted in a round-bottomed glass reactor of 2 l volume (height 25 cm, diameter 10.5 cm) with four stainless steel bafflers (width 1.5 cm) placed inside to ensure thorough stirring. The Teflon cover had inlets for a reflux condenser, a stirring rod (with 4 sets of 4 tilted paddles), a thermosensor, a gas tube and two electrodes. The chosen temperature was maintained by a flexible electric heating cover placed around the vessel. A signal from the thermosensor placed inside the reaction vessel was used to adjust the heating power of the cover according to the chosen temperature. Nitrogen feed was used to ensure an oxygen free environment. In the potentiometric experiments, a platinum electrode was used as the working electrode and a commercial Ag/AgCl- electrode (REF 201 / Radiometer, 0.197 V vs. NHE at 25 °C) as the reference. All potentials are given against the Ag/AgCl electrode. A picture and a schematic of the apparatus are given in Figures 2 and 3.

Figure 2. A picture of the dissolution reactor.

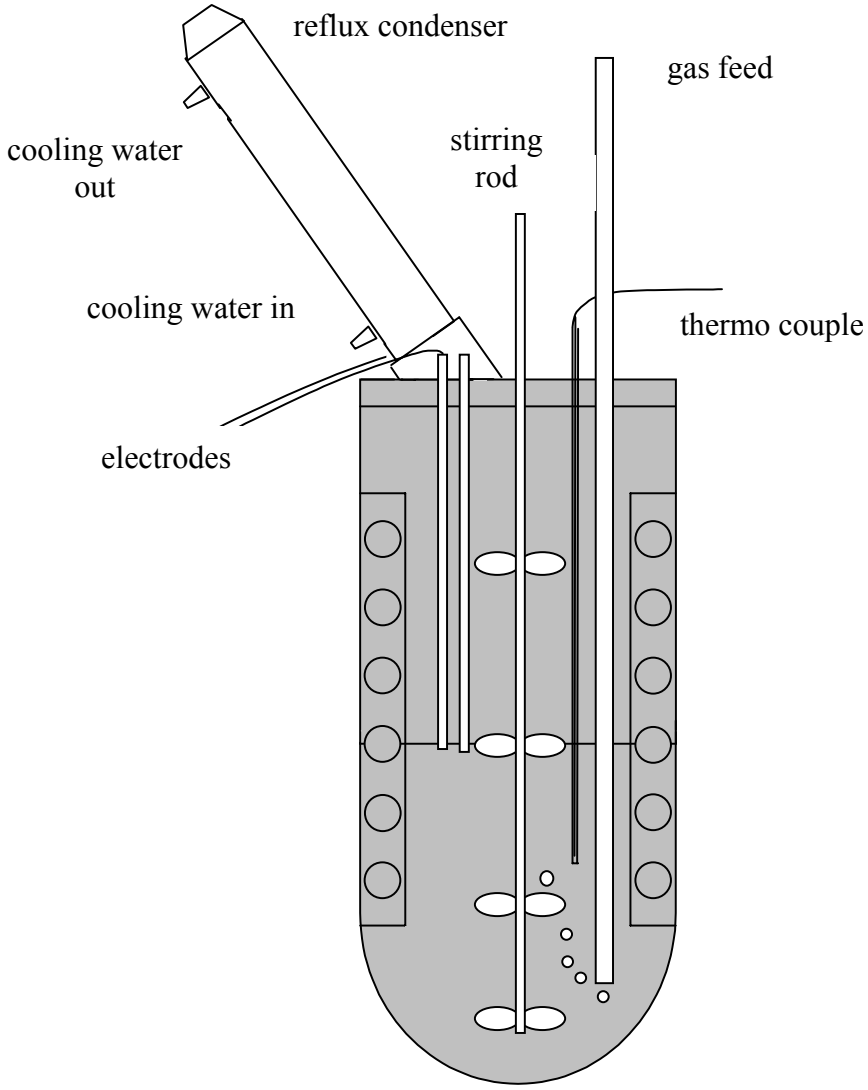

Figure 3. A schematic of the dissolution reactor.

6.3 PROCEDURE

1.5 l of sulphuric acid (0.2 M or 20g/l) was used in each measurement. The acid was preheated and poured into the reaction vessel, and ferric sulphate and/or MnO_2 was added. Nitrogen was bubbled through the solution for 15 minutes before and throughout the measurement to ensure an oxygen-free environment. After oxygen had been removed and the temperature of the solution had stabilised at 80 °C, the zinc concentrate was added to the solution. The solutions were

stirred at a constant rate to keep the solid matter in solution. Samples taken at given intervals were filtered and analysed with AAS to determine the conversion of zinc.

The ability of manganese dioxide to dissolve the sulphide was studied in both solutions containing and not containing iron. Under study were the galvanic interactions between the concentrate and the oxidant as well as the interaction between MnO_2 and iron. Also of interest was whether the MnO_2 could dissolve the elemental sulphur layer forming on the particle surfaces. The measurement parameters are presented in Table 1.

Table 1. Measurement parameters.

No.	ZnS (g/l)	Fe^{3+} (g/l)	MnO_2 (g/l)	t (min)
1	2	2.4	4.5	300
2	2	2.4	22.6	300
3	2	0	4.5	300
4	2	0	22.6	300
5	10	0	20	300
6	10	4.4	0	480
7	10	0	20	480
8	10	4.4	20	480
9	10	0	20	600

To study the effect of MnO_2 on ferrous ions, a solution of 4.2 g/l Fe^{2+} was made into oxygen-free 0.2 M sulphuric acid. Solid MnO_2 (20 g/l) was introduced into the system and the potential was recorded as a function of time. Nitrogen was fed throughout the measurement. Samples of the solution were extracted and titrated with potassium dichromate solution to determine the amount of Fe^{2+}. The sodium salt of diphenyl amino sulphonic acid was used as the indicator.

6.4 RESULTS AND DISCUSSION

6.4.1 Dissolution efficiency of MnO_2 and Fe^{3+}

Figure 4 shows the conversions of zinc as a function of time in solutions containing 0 or 2.4 g of Fe^{3+} and 0, 4.5 or 22.6 g of MnO_2 per litre of acid. All solutions contained 2 g/l of ZnS concentrate. When MnO_2 was the only oxidant, conversions remained low, with the lower MnO_2 content giving a conversion of 9 % and the higher 15 % after 300 minutes. In the solution containing only ferric iron as the oxidant, conversion was close to 50 % after the same time. The ferric iron was considerably more effective an oxidant, due to it being dissolved in the solution whereas oxidation by MnO_2 depends wholly on galvanic contacts.

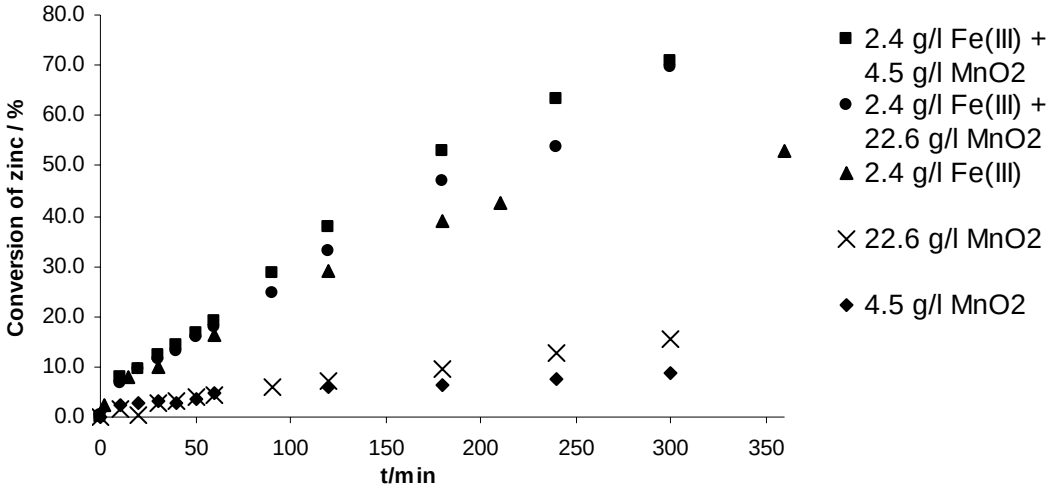

Figure 4. Conversion of zinc in 0.2 M sulphuric acid with varying amounts of MnO_2 and Fe^{3+} and 2 g/l ZnS at 80°C.

Figure 4 also shows the combined effect of the two oxidants. The addition of MnO_2 into a solution containing Fe^{3+} increased conversion by almost 20 %, whereas the amount of MnO_2 addition (4.5 or 22.6 g) seemed to make little difference. However, the combination of the two oxidants resulted in higher conversions than the sum of the two separate reactions. This suggests, that a rapid oxidation reaction took place between the ferrous ion and MnO_2, replenishing the solution with ferric ions. As the concentration of ferric ions remained high

throughout the measurement, the reaction continued faster than in the case with no reoxidisation of iron.

Although the dissolving effect of magnesium dioxide was evident, the low amount of the solids resulted in a low number of galvanic contacts and the conversions remained low. Figure 5 shows how the increase in solids affected the conversion of zinc. It can be seen, that increasing the amount of MnO_2 fivefold increased the conversion only by 6 %, whereas increasing the amount of concentrate fivefold increased the conversion by 36 %.

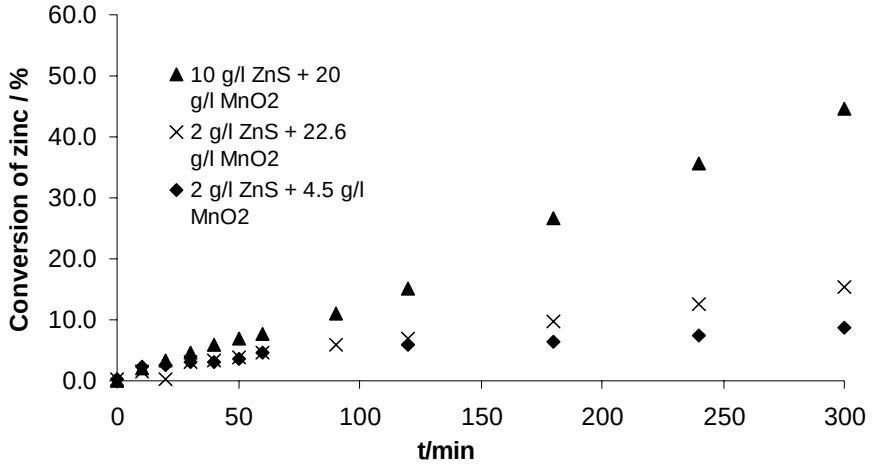

Figure 5. The effect of the amount of solids on the conversion of zinc in 0.2 M sulphuric acid at 80°C.

Figure 6 shows the results of dissolution experiments with a higher ZnS content. In a solution with 10 g/l of concentrate and 20 g/l of MnO_2, conversion at 300 minutes was close to 50 %. In the experiment with only Fe^{3+} as the oxidant, the reaction stopped after 40 % conversion is reached, as all ferric iron had been reduced to the ferrous form and there was no other oxidant present to oxidise the iron or the concentrate. The conversion obtained by the addition of these two effects exceeded the actual conversion from an experiment with both of the oxidants present. This due to the high amount of oxidants and the high conversions reached. The dissolution slowed down as the availability of unreacted concentrate was strongly reduced.

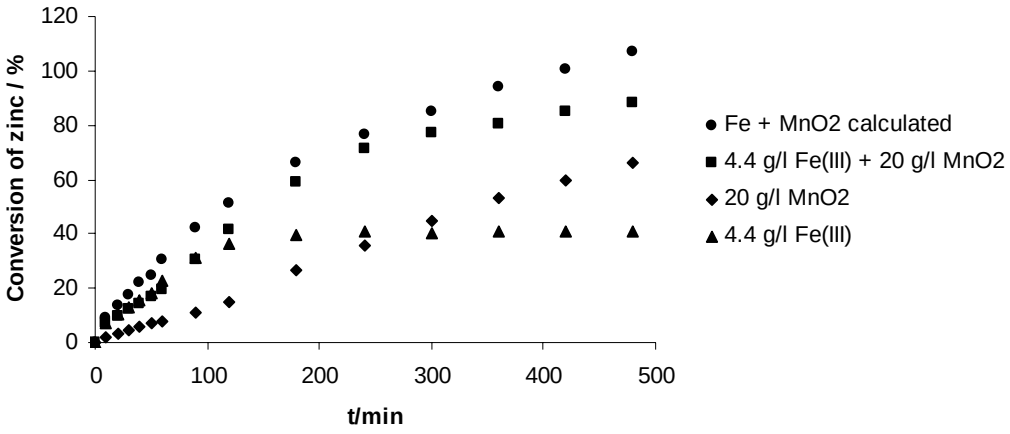

Figure 6. Conversion of zinc in 0.2 M sulphuric acid with 0 or 20 g of MnO_2 and 0 or 4.4 g of Fe(III) in the solution (10 g/l ZnS) at 80°C.

6.4.2 The effect of MnO_2 on ferrous ions

Analysis was also made to determine the degree of MnO_2 dissolution. The amount of dissolved Mn as a function of time is depicted in Figure 7. When only ZnS and MnO_2 were present in the solution, the rate of dissolution was constant, giving a 30 % conversion after 6 hours. When ferric ions were added, the reaction rate was faster, but not equally linear, giving a conversion of 45 % at 6 h. The reduction in dissolution rate was due to the depletion of ferrous iron as there was not enough of the species to oxidise all of the MnO_2. However, as the dissolution of manganese dioxide was enhanced by the presence of ferric ion, a direct reaction between the species was suggested, according to reaction 32:

$$2\ Fe^{2+} + MnO_2 + 4\ H^+ \rightarrow 2\ Fe^{3+} + Mn^{2+} + 2\ H_2O \qquad (32)$$

The reaction was studied by monitoring the potential of a solution with only MnO_2 and Fe(II) present in the beginning, as the potential of the solution is determined by the Fe(II) to Fe(III) ratio. The potential of the iron-(II) - sulphuric acid solution at 80 °C was 400 mV vs. Ag/AgCl. The change in potential after MnO_2 was introduced into the system can be seen in Figure 8.

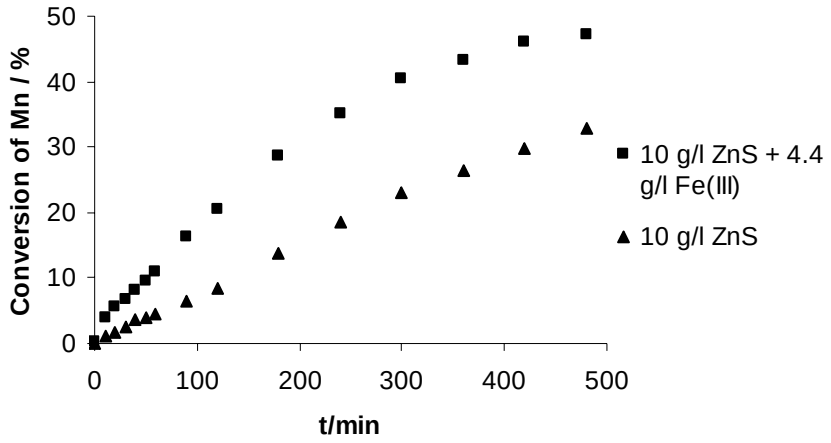

Figure 7. Conversion of manganese in 0.2 M sulphuric acid with 10 g of ZnS and 0 or 4.4 g of Fe(III) in the solution (20 g/l MnO_2).

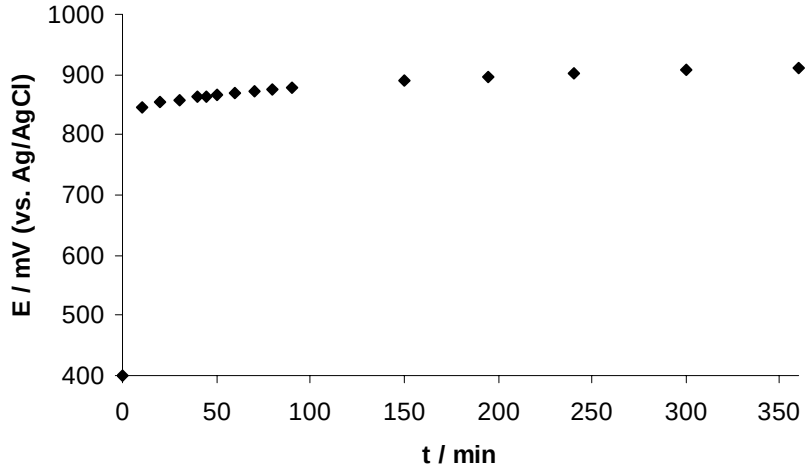

Figure 8. The potential of the solution as a function of time in a reaction between Fe(II) (4.2 g/l) and MnO_2 (20 g/l) in sulphuric acid .

In the beginning of the measurement Fe(III) was present only in minute amounts. The MnO_2 in the solution rapidly oxidised the ferrous ions into the ferric form, which can be seen as a rise in the potential. These results were confirmed by the titration of solution samples. After the first few samples, the presence of Fe(III) could be seen directly from the indicator colour in the solution, which had a smooth transition from yellow (first 30 min) via reddish brown (45 min) to dark purple (> 50 min) indicating the change in the valence of the iron species.

6.4.3 The effect of MnO_2 on elemental sulphur

When ferric ions are used to dissolve sphalerite, the rate of dissolution is reduced after a few hours. This is due to the elemental sulphur layer forming on the surfaces of the particles. When MnO_2 was used for the dissolution, the reaction rate remained constant, which could be interpreted as the dissolution of the sulphur layer. Figure 9 shows the amounts of Zn and Mn dissolved during a 10-hour experiment. If equation (29) was obeyed, the molar amounts dissolved should be equal. As is seen, MnO_2 was used up in excess, suggesting a parallel reaction, such as the dissolution of the sulphur layer according to equation 33:

$$3\ MnO_2 + S^0 + 4\ H^+ \rightarrow 3\ Mn^{2+} + SO_4^{2-} + 2\ H_2O \qquad (33)$$

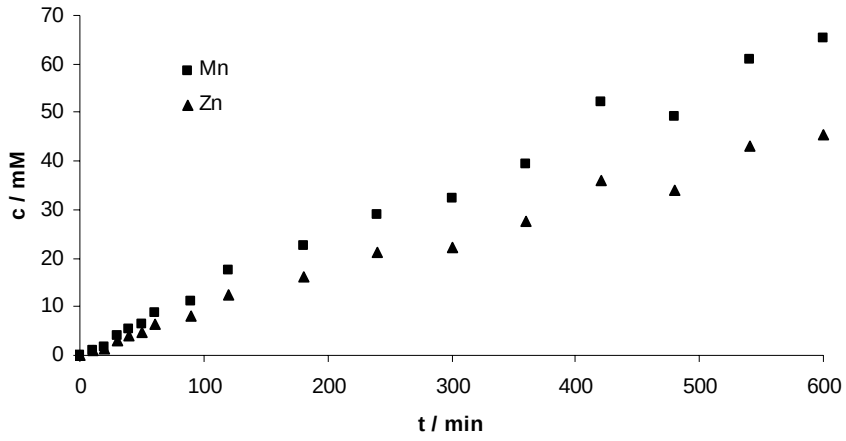

Figure 9. The amount of dissolved Mn and Zn during dissolution in 0.2 M sulphuric acid at 80 °C, with 10 g/l of concentrate and 20 g/l of MnO_2.

To determine whether the elemental sulphur layer was dissolved or not, samples of the concentrate before and after dissolution were analysed for Mn, Zn and S. The weight percentages of sulphur in the residue are presented in Figure 10. The zinc conversions calculated from the solution analysis results were used to calculate the expected values for the sulphur weight percentages, assuming that no sulphur was dissolved. As is seen, the fraction of sulphur in the concentrate residue was decreased during dissolution with MnO_2. If the elemental sulphur

layer was inert to oxidization in these conditions, the fraction of sulphur in the residue should grow, as zinc is leached out of the concentrate. It has to be noted however, that the changes in total mass and in the percentages of sulphur were small.

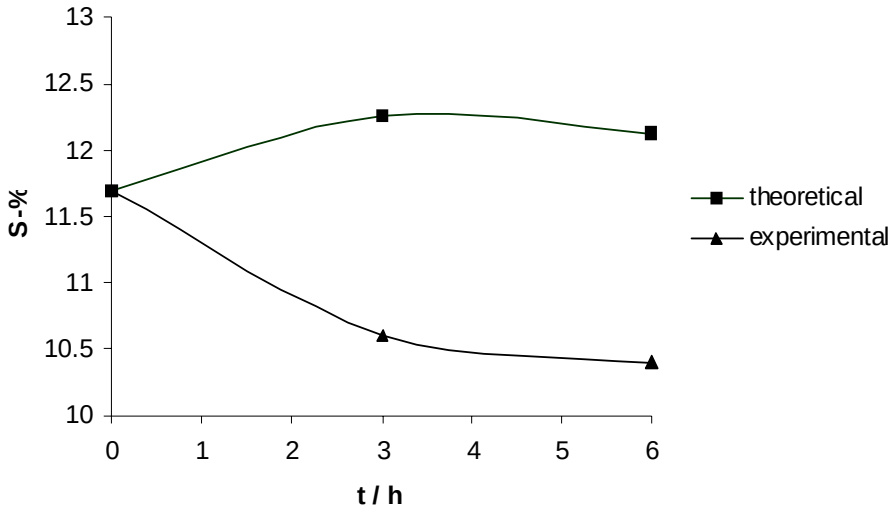

Figure 10. The weigh-percentage of sulphur in dissolution residues, calculated and experimental.

In conclusion, it was found that MnO_2 affects the dissolution of sphalerite by two mechanisms: by directly oxidising the sulphur in the mineral and by regenerating the active ferric species. When MnO_2 was the only oxidising species in the solution, the dissolution proceeded linearly with time, which suggests further oxidation of the elemental sulphur layer. This was also suggested by the results showing an excess of MnO_2 dissolution compared to the stoichiometric amount required by the sphalerite oxidation. Analysis of sulphur in the dissolution residue also corroborated the theory of further sulphur oxidation.

7 DISSOLUTION EXPERIMENTS WITH FERRIC IONS

Batch dissolution experiments were conducted to study the dissolution behaviour of two sphalerite concentrates using ferric ions as the oxidant. Measurement parameters were chosen to match those in industrial scale dissolution. The goal was to simulate the industrial process and find out how different parameters affect the rate of dissolution.

7.1 MATERIALS

The composition of the sphalerite concentrates used, Concentrate B and Concentrate C, are shown in Table 2. Fractions with diameters > 37 µm and < 37 µm were used. Sulphuric acid solution was diluted from concentrated H_2SO_4 (Merck) with MilliPore ion-exchanged distilled water. The ferric, cuprous and zinc sulphates (Riedel-de Haën) were of reagent grade.

Table 2. The composition of Concentrate B and Concentrate C fractions and their surface areas.

	Size	% Zn	% S	% Fe	% Pb	% Cu	m2/g
B1	<37µm	53.7	13	5.9	1.3	1.3	1.11
B2	>37µm	54.8	9	4.4	1.1	1.1	0.632
C1	<37µm	53	36	9.8	1.4	1.4	0.868
C2	>37µm	52.8	29	10.1	1.4	1.4	0.525

7.2 EQUIPMENT

The measurements were conducted in a new reactor, the dimensions of which were more suited for modelling purposes. The reactor had a level bottom, and the stirring rod was changed to a standard 4-paddled one. Otherwise the reactor was identical to the one used in the MnO_2 dissolution experiments.

7.3 PROCEDURE

The sulphuric acid was preheated and sulphates of iron, zinc and copper were introduced to the system. After the temperature had stabilised, the concentrate was added. Oxygen was fed to the system 15 minutes prior and throughout the experiment. After the chosen reaction time, the residue was filtered, washed with MQ-water, dried and analysed with AAS. Conversion of zinc under different conditions could be calculated from the analysis results.

The conditions in these measurements were closer to real values in the industrial zinc process than in previous measurements done for the master's thesis of Aaltonen [46]. The chosen parameters were temperature (80 °C and 95 °C), solution iron content (8 g/l and 25 g/l) and zinc content (60 g/l and 120 g/l), sulphuric acid concentration (20 g/l and 80 g/l), concentrate (Concentrate B and Concentrate C) and the concentrate fraction (< 37 µm and > 37 µm). In all measurements, the amount of concentrate was 10 g/l and the reaction time was 3 hours. Table 3 shows the measurement plan for one concentrate fraction. Differing values were used for some of the preliminary experiments described in sections 7.4.1 – 7.4.3.

A preliminary study showed, that copper in the solution affects the dissolution process and as there is always some dissolved copper in the industrial process, 1 g/l of copper was added to all solutions. All solutions containd 60 g or 120 g of zinc sulphate per litre. The amount of zinc entering the solution from the dissolving concentrate was very small compared to this and could not be analysed reliably from the solution. Analysis had to be made from the concentrate residue, which made the sampling considerably more difficult than in prior experiments.

Table 3. Measurement plan for one concentrate fraction.

Measurement	T/C	m(Fe)/(g/l)	m(Zn)/(g/l)	m(acid)/(g/l)
1	80	8	120	80
2	80	8	60	20
3	80	25	120	20
4	80	25	60	80
5	80	25	60	20
6	80	8	120	20
7	80	8	60	80
8	80	25	120	80
9	95	8	120	20
10	95	25	60	20
11	95	8	60	80
12	95	25	120	80
13	95	8	60	20
14	95	25	120	20
15	95	25	60	80
16	95	8	120	80

7.4 RESULTS AND DISCUSSION

7.4.1 Sampling

The solutions contained plenty of zinc and the analyses had to be done from the dissolution residue. The plan was to use the lead in the concentrate as an internal reference, which could be used to calculate the conversion of zinc without knowing the total mass of undissolved concentrate at a given time. For this to succeed the lead had to be inert and remain in the residue. Part of the solution would be filtered through a membrane and the small sample of solids analysed.

To determine the reliability of this method, a series of measurements was conducted where the results of samples taken during a measurement were compared with the results of batch dissolution experiments. In the batch experiments the entire undissolved residue was filtered, washed, dried and weighed prior to AAS analysis, giving the absolute amount of undissolved zinc. Parallel analyses of the residue were made at the laboratories of Outokumpu Research Oy (ORC) and Analyysikeskus.

The results of the batch dissolution experiments as analysed in ORC and Analyysikeskus are depicted in Figure 11 for the zinc content and Figure 12 for the lead content. The zinc content decreased with time, as was expected and the results of the two laboratories correlated well. Also, the lead analyses were congruent, but the lead did not behave as expected. The lead seemed to be active during the experiments and the amount of lead in the residue varied with time.

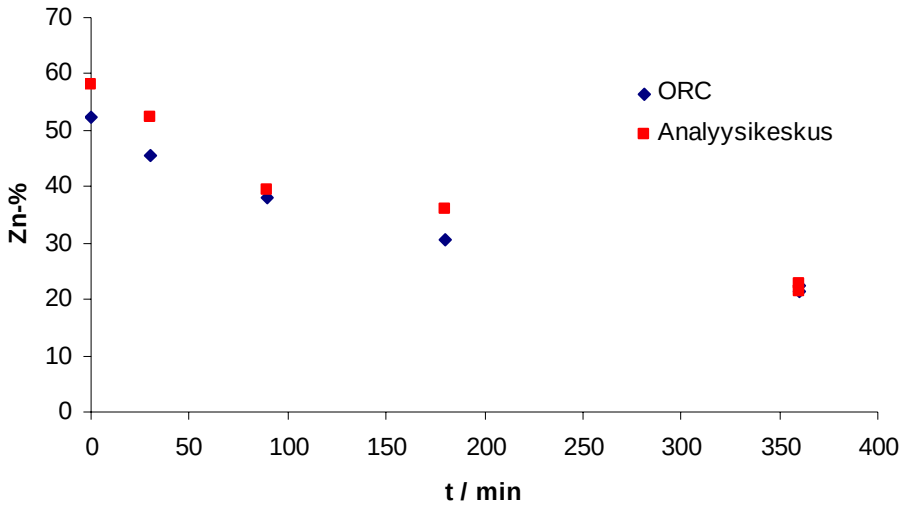

Figure 11. The zinc content of the residue as a function of leaching time in 0.2 M sulphuric acid with 8 g/l of ferric iron and 10 g/l of concentrate. Results from the laboratories of ORC and Analyysikeskus.

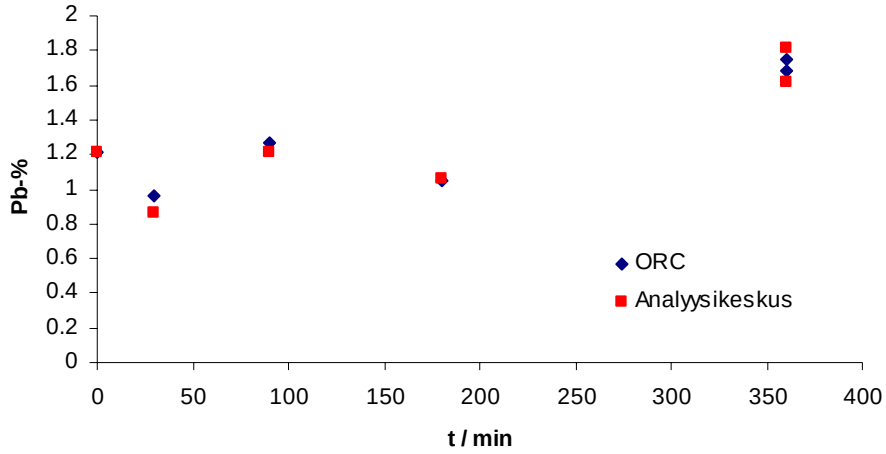

Figure 12. The lead content as a function of leaching time in 0.2 M sulphuric acid with 8 g/l of ferric iron and 10 g/l of concentrate. Results from the laboratories of ORC and Analyysikeskus.

Figure 13 shows the lead / zinc –ratios as a function of time for the measurements with the two different sampling methods. The higher curves had been analysed from the batch experiments in both laboratories, the lowest curve was calculated from the small samples taken during a longer measurement and analysed at Analyysikeskus. The ratio clearly varied with the method of sampling. The difference in the analysis results of the various methods was 10 % for the zinc and 90 % for the lead.

The taking of samples during the measurement was made very difficult by the inhomogeinity of the solution and it was almost impossible to get a representative sample. The elemental sulphur layer forming on the surfaces is hydrophobic and reacted particles rose to the surface. This separation of particles was advanced by differences in mass. Also, in the feeding of the concentrate to the solution, the concentrate tended to remain on the surface and not mix throughout the reactor. Some of these problems were solved by mixing the concentrate in a small amount of acid, thus wetting it, before pouring it into the reactor. The use of lignosulphonate and an anti-foaming agent also considerably increased the homogeinity of the solution. However, the difference between the two sampling

methods remained too big and the experiments had to be conducted as batch measurements, where the entire residue is weighed and analysed.

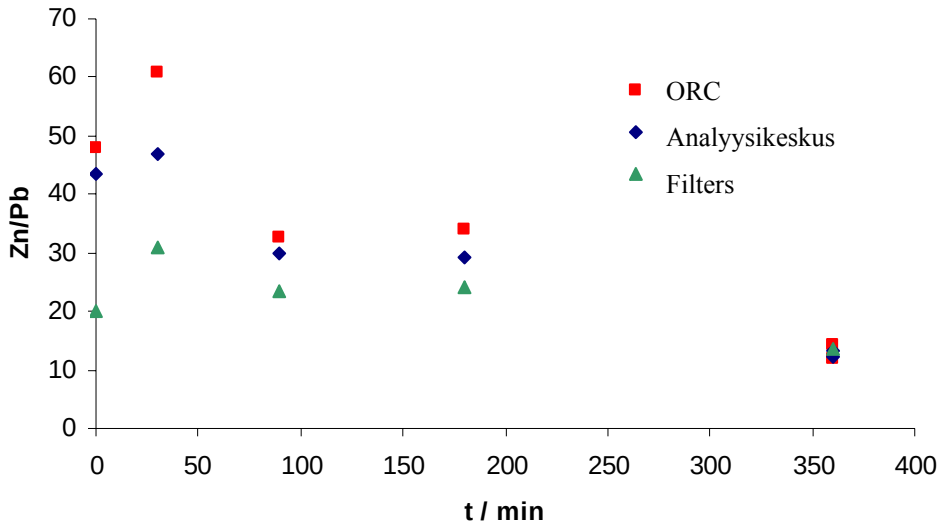

Figure13. The zinc/lead-ratio as a function of leaching time in 0.2 M sulphuric acid with 8 g/l of ferric iron and 10 g/l of concentrate. Results form full residue analysis (ORC and Analyysikeskus) and from intermediate sample analysis (Filters).

Figure 14 shows the zinc conversions calculated by different methods as a function of time. The two lower curves show the conversion calculated from the Zn/Pb-ratio and as can be seen, they clearly differ from the expected continually increasing form. The higher curves are calculated by using only the zinc contents of the residues, assuming that all the change in mass is due to zinc passing into the solution from the lattice. These curves are much closer to the ones expected for a dissolution reaction than the previous ones. Naturally this assumption is not acceptable when gathering quantitative data, but the figure shows, that even crude assumptions result in better agreement with theory and other experiments than using lead as an internal standard.

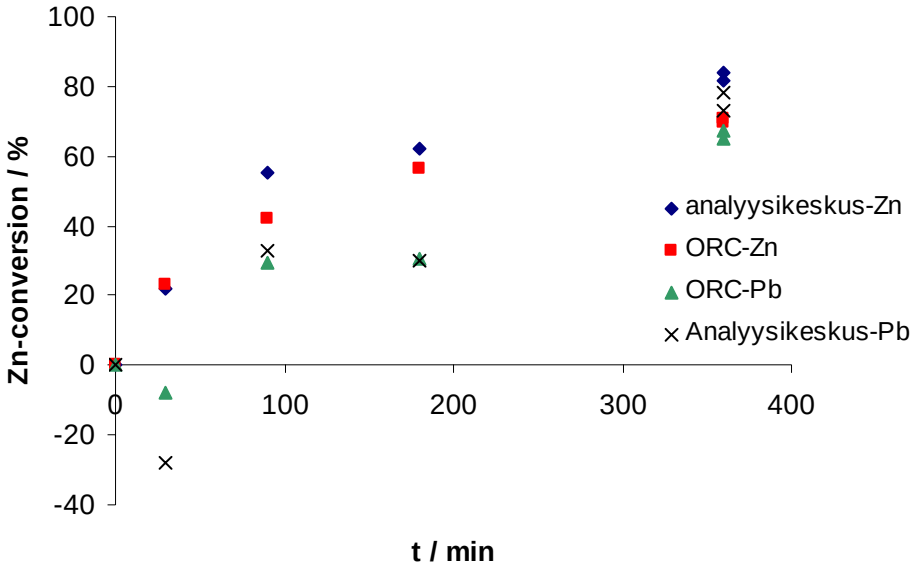

Figure 14. The conversion of zinc as a function of leaching time in 0.2 M sulphuric acid with 8 g/l of ferric iron and 10 g/l of concentrate, calculated from the residue zinc analysis (-Zn)(assuming only zinc dissolves) and from the Zn/Pb-ratio (-Pb). Results from the laboratories of ORC and Analyysikeskus.

7.4.2 The effect of copper

The industrial solutions contain copper, so the effect of copper on the oxidation of ferrous iron was studied. Oxygen was fed to a sulphuric acid solution containing ferrous iron and the potential was recorded, as a rise in the solution potential indicates the formation of ferric ions. This can be deduced from the Nernst equation:

$$E = E^0 - \frac{RT}{nF} \ln \left[\frac{Fe^{3+}}{Fe^{2+}} \right] \qquad (34)$$

where E is the solution potential, E^0 the standard equilibrium potential, R, T, n, and F have their usual meanings and $[Fe^{3+}]$ and $[Fe^{2+}]$ are the concentrations of the ferric and ferrous ions, respectively.

Figure 15 shows the change in potential in a solution without copper and with 1 g/l of copper. Copper greatly increased the rate of ferrous oxidation as could be seen from the changes in potential. This effect was subdued in a solution containing a zinc base (60 g/l), but since copper did affect the kinetics of the oxidation, 1 g was added to all solutions.

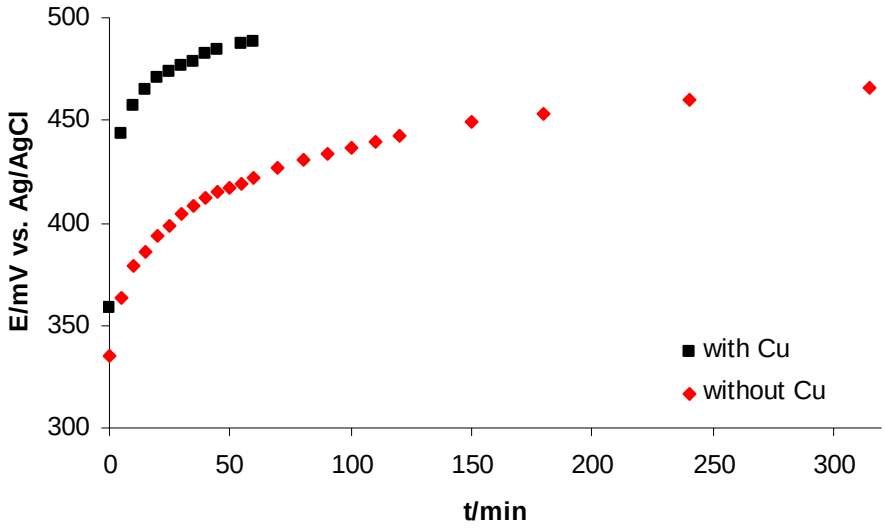

Figure 15. The effect of copper on ferrous ion oxidation with oxygen in 0.2 sulphuric acid at 80°C.

7.4.3 Solution potential

The solution potential was determined by the ratio of ferric to ferrous ions according to equation (34). The solution potential was to be controlled separately from the total concentration of iron by oxygen feed; so two iron concentrations could be studied at two potentials. Figure 16 shows the potential as a function of time for a solution with 15 g/l of concentrate, 8 g/l of iron, 60 g/l of zinc in 0.2 M sulphuric acid at 80°C as oxygen is fed throughout the measurement. The oxygen was not enough to stop a change in potential. The experiment was repeated with identical results. The great potential drop in the beginning of reaction was caused by a small change in concentrations, due to the logarithmic nature of the potential, and could be eliminated by adding some ferrous sulphate to the solution prior to

the experiment. However, the potential continued to decrease for several hours before equilibrium was reached.

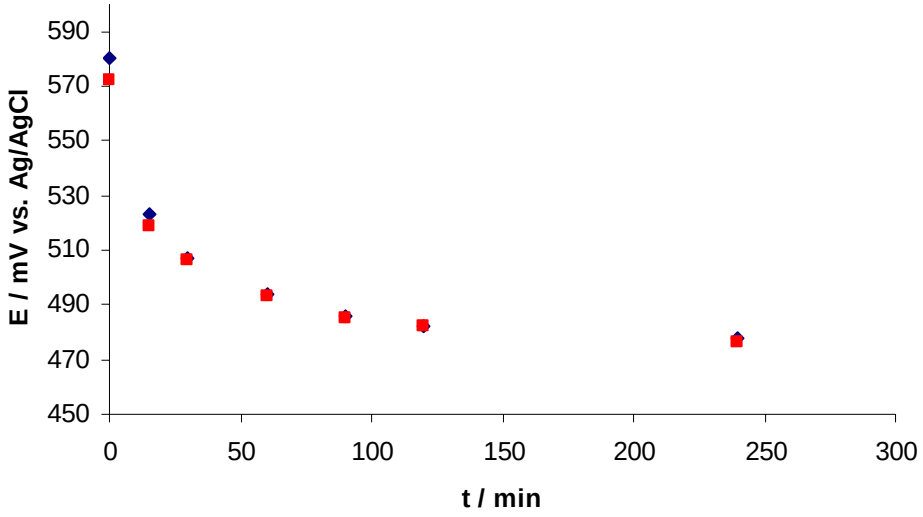

Figure 16. Solution potential as a function of time for a dissolution experiment in 0.2 M sulphuric acid solution with 15 g/l of concentrate, 8 g/l of iron and 60 g/l of zinc at 80°C.

Figure 17 shows the results of oxidation experiments where the effects of mixing, oxidation and amount of concentrate were studied. The highest curve is from a measurement with only 3 g/l of concentrate; the other measurements had 15 g/l. As expected, the lower concentrate content resulted in a smaller potential drop, as there was less of one reactant resulting in a slower overall reaction. The two curves in the middle show the effect of mixing, the higher curve being from a measurement with mixing at 300 rpm, the lower at 800 rpm. It can be seen, that the effect of low mixing in slowing down the reaction was greater than the effect of increased mixing on oxygen dissolution. The lowest curve represents the measurement without oxygen feed and in this case the potential continued to decrease throughout the measurement. The other measurement parameters remained constant.

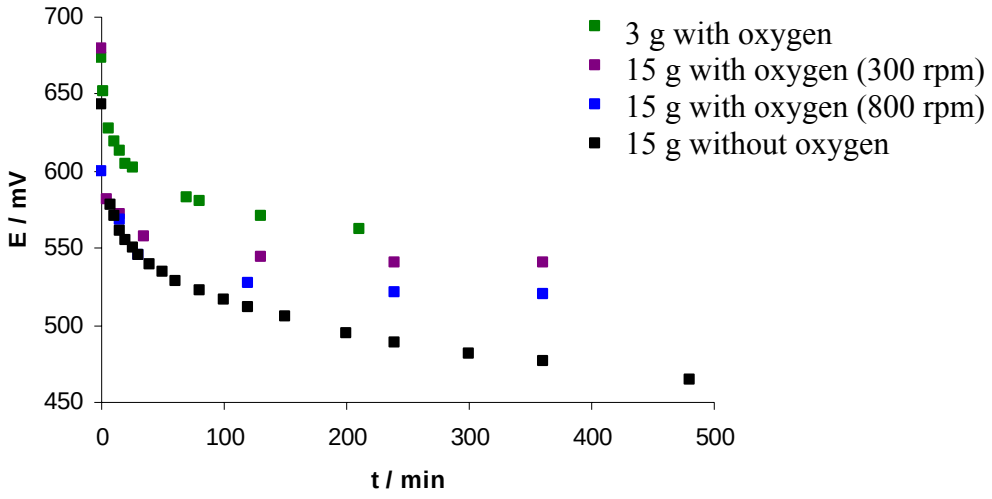

Figure 17. The effect of stirring, amount of concentrate and oxygen feed on the solution potential as a function of time, for a dissolution experiment in 0.2 M sulphuric acid solution with 3 or 15 g/l of concentrate, 8 g/l of iron and 60 g/l of zinc at 80°C, with or without oxygen feed.

Figure 18 shows the effect of selected solution parameters on the potential of the solution. The basic values were 8 g/l of iron and 60 g/l of dissolved zinc in the solution. The higher values were 25 g/l for the iron (Fe+) and 120 g/l for the zinc (Zn+). The basic measurement was done as a 1 hour and as a 6 hour experiment, and the correlation between the solution potentials can also been seen in Figure 18. The measurements did seem to have good repeatability, as the two basic measurements quickly converge on the same potential trend. The differences in potential in the beginning of the measurements were caused by very small changes in concentrations. As expected, the higher amount of iron(III) raised the solution potential. The zinc had a similar effect, only to a lesser extent. This could be due to the additional zinc slowing down the dissolution reaction, thus keeping the solution potential at higher values.

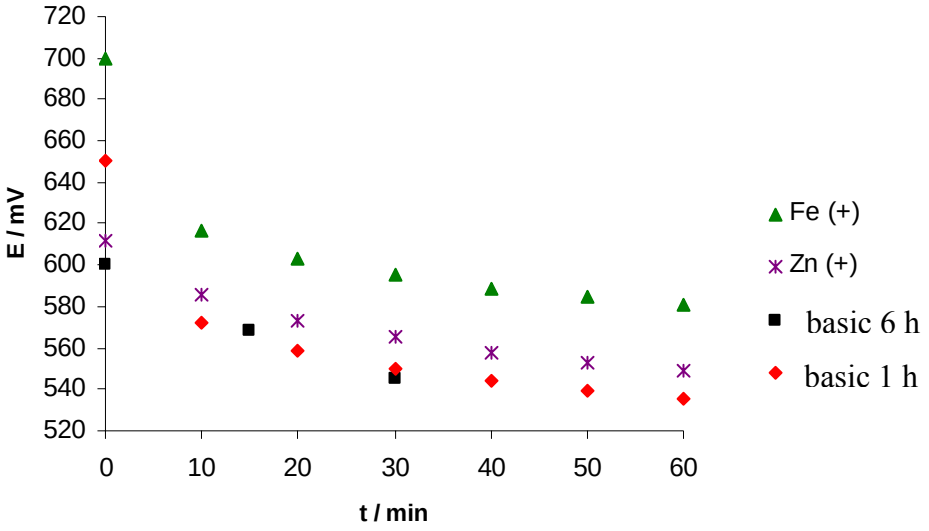

Figure 18. The effect of solution parameters on the solution potential for experiments with 10 g/l of concentrate, 8 or 25 g/l iron and 60 or 120 g/l of zinc in 0.2 M sulphuric acid at 80°C.

The oxygen feed was maximised in order to stop the continuous decline in potential, but in a small reactor with no mentionable hydrostatic pressure, the dissolution of oxygen and the consequent oxidation of ferrous iron took place more slowly than the reduction of iron caused by the concentrate. With no adequate way of oxidization, the outside potential control was left out of the measurements, and oxygen was fed into the system only to minimize the change in potential. The potential level of the solution was thus determined by the amount of ferric ion fed to the system.

7.4.4 Batch dissolution experiments

The results of the 64 measurements are given in Appendix 1. The effects of particle size, temperature and iron, zinc and acid concentration on the conversion of zinc under differing conditions are expressed in Appendices 2-11. The tables express the measurement parameters and the graphs show the effect of the variable in question. The effects are shown separately for the two concentrates under study, Concentrate B and Concentrate C, and a comparison of both fractions

of both concentrates are shown in Appendix 12, where the parameters are given by Table 3 on page 40.

The most pronounced effect on the conversion of zinc was by the size fraction of the concentrate. For the Concentrate B, the conversions for the smaller fraction were by average 27 mass percent higher than for the fraction with the larger particle size. The corresponding result for the Concentrate C was 21 mass percent. The average conversions for the four fractions are given in Table 4, along with the particle sizes and specific surface areas. As expected, the concentrate fraction with the highest specific surface area had the highest conversion and the conversions decreased with decreasing surface area. The differences between the two concentrates in copper and iron concentration seemed to have less effect than the surface areas. Once the conversions were divided by the surface area of the concentrate in question (in m^2/g), to give a scaled conversion, the average conversion for the Concentrate C was 15 m-% higher than the one for Concentrate B. This could be due to the increased concentration of iron in the lattice.

Table 4. The conversions (X), particle sizes and surface areas of the used concentrates.

Fraction	Size	A (m2/g)	X / m-%	X/A
B1	<37µm	1.11	74	67
B2	>37µm	0.632	47	74
C1	<37µm	0.868	62	71
C2	>37µm	0.525	45	86

Increasing the temperature from 80 °C to 95 °C raised the average conversion of the Concentrate B by 15 m-%, with two of the measurements showing decrease in conversion. The results for the Concentrate C were more varied, with 5 out of 16 measurements showing a decrease in conversion with the increase in temperature. For the experiments with a positive effect, the average increase was 11 m-%, the total effect being only a 3 % increase.

The concentration of iron in the solution also had a clear effect on the conversions. The conversion for the Concentrate B was increased by 11 m-% and of the Concentrate C by 7 m-% by the increase of ferric iron from 8 to 25 g/l. The effects of the acid and zinc concentrations were negligible on the conversion reached at Concentrate B dissolution, with an average difference of 1 m-%. The effects on the Concentrate C were slightly stronger, with average effects of 5 m-% and 2 m-% respectively. The error in the measurements was studied by repeating 10 of the measurements as shown in Appendix 13. The average error was found to be 3 m-%. Therefore the only considerable effects were those of size fraction, temperature and the iron concentration.

8 ROTATING RING-DISC ELECTRODE

A rotating ring disc electrode was constructed, in which a pressed concentrate pellet was used as the disc. The Fe^{2+} ions formed by the dissolution of ZnS in the disc were detected on the platinum ring by oxidising them back to the ferric form. The measured current was used to determine the rate of dissolution. The method can be used to study the kinetics of dissolution in the very beginning of the reaction, before a layer of sulphur is formed on the surface. The method is fast and can thus be used for rapid comparison of the dissolution characteristics of different concentrate fractions.

8.1 MATERIALS

The Concentrate B <37 μm fraction was used. Sulphuric acid solution was diluted from concentrated H_2SO_4 (Merck) with MilliPore ion-exchanged distilled water. The ferric, cuprous and zinc sulphates (Riedel-de Haën) were of reagent grade.

8.2 EQUIPMENT

The rotating ring disc electrode consisted of a 1 mm thick platinum ring (inner diameter 15 mm), inside which is a 1 mm layer of insulator and then a space for a 13 mm disc electrode. The exchangeable disc electrode pellets were mechanically pressed from the concentrate with sulphur (6 m-%) as the binder. The top and side views of the electrode are shown in Figure 19 and a picture of the set-up in Figure 20. The counter electrode was a platinum net and the reference a commercial Ag/AgCl-electrode (REF 201 / Radiometer).

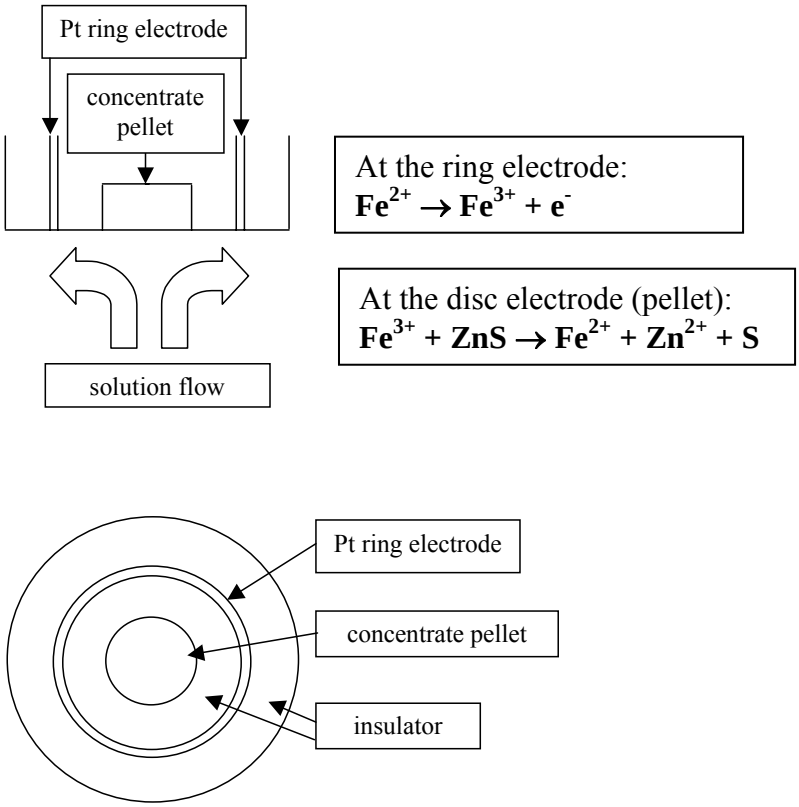

Figure 19. A schematic of the RRDE.

Figure 20. A picture of the RRDE-equipment.

8.3 PROCEDURE

In the basic measurements the acid concentration was 0.2 M, the iron concentration 8 g/l and the temperature 80 °C. To study the effect of temperature, this parameter was changed to 60, 70 and 90 °C. The effect of iron was studied by increasing its content to 25 g/l, the effect of acid by increasing the concentration to 0.8 M and the effect of copper by adding 1 gram of it per litre. All measurements were repeated at 5 rotation speeds: 5, 10, 15, 20 and 25 Hz.

The measurements were conducted in a three-necked flask, with 0.25 l of solution. The flask was warmed with an adjustable heater connected to a thermosensor in the flask through a controlling device. The solution was heated and the electrode set down in the acid and set to rotate. Iron was introduced to the solution, once everything else was set, to ensure the recording of current from the very beginning of dissolution.

8.4 RESULTS AND DISCUSSION

8.4.1 Experimental results

The plan was to do the RRDE measurements in solutions alike those in the real industrial process. The response was good in sulphuric acid when no zinc had been added, but the presence of zinc greatly disturbed the signal. The measurements had to be done in solutions without dissolved zinc. Figure 21 shows the ring current in 80°C sulphuric acid (0.2M) with 8 or 25 g/l of ferric iron. The increase in current caused by the increased amount of iron was clearly evident. Thus this method is applicable to study the effect of different variables on the dissolution kinetics of the concentrate. Appendix 14 shows pictures taken of the pellet surface before an experiment (3a,0) in 80°C sulphuric acid (0.8M) with 8 g/l of ferric iron, after measurement at various rotation rates (after 7 minutes, 3a,k) and after 12 minutes of dissolution (3a,l). After 7 minutes the previously smooth surface had become rougher and the formation of an island of elemental sulphur was seen. After 12 minutes of dissolution, further cracking of the surface

was noted. However, the pellet remained intact and repeatable electrochemical experiments could be conducted.

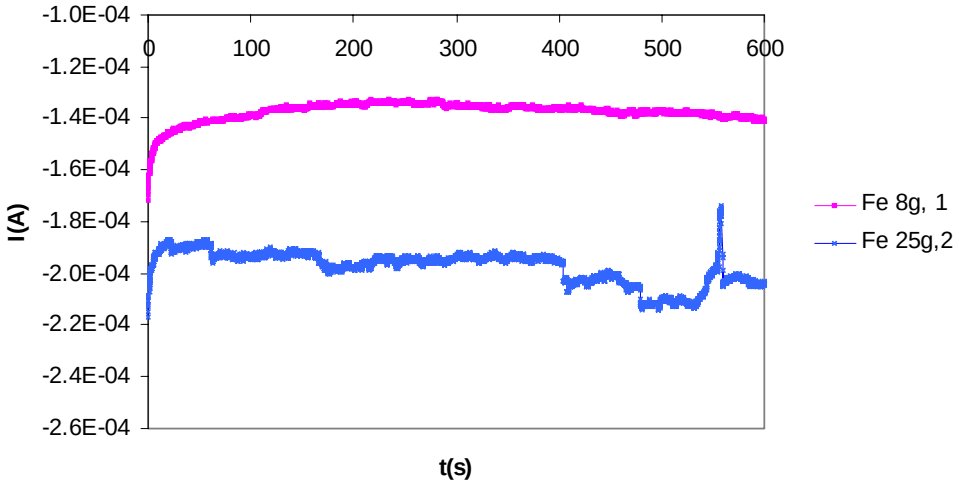

Figure 21. Current of the ring electrode as a function of time. The temperature is 80 °C, concentration of sulphuric acid 0.2 M and the amount of iron in solution 8 or 25 g/l.

Figure 22 shows the effect of temperature on the rate of dissolution. The inverse of the ring current is shown as a function of the square root of the angular speed, so that the value of kinetic current is obtained by extrapolation. (Only the magnitude of the current has been considered in Figures 22-24, the negative sign has been omitted.) Thus, the effect of kinetics and transport processes on the current can be separated, allowing a closer look on the factors affecting the kinetics of the reaction. The slopes of the extrapolated lines in Figure 22 suggest that the reaction mechanism at 60°C differs from that at higher temperatures. This is in accordance to earlier results [46]. However, the possibility of a measurement error has to be considered, as the extrapolated current at infinite mass transfer lies in the negative region. A definite difference in the rates of reaction can be seen between the measurements at higher temperatures.

Figure 23 shows the effect of copper on the dissolution process and it is seen that in solutions with copper the dissolution rates were less dependent on the rate of

diffusion than in solutions without copper. Possibly the copper oxidised the ferrous ions and diffusion of ferric ions from further in the solution was no longer rate-determining. In contrast, Figure 24 shows that the concentration of the sulphuric acid had practically no effect on the dissolution, at least not in this concentration range. These were a preliminary set of measurements to test the applicability of this method in the study of concentrate dissolution kinetics.

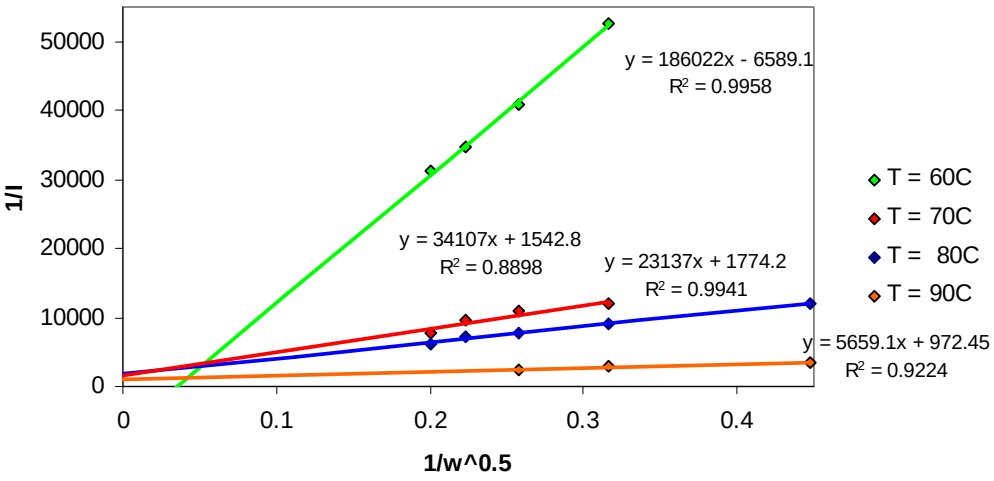

Figure 22. The inverse of the ring current as a function of the square root of the angular speed. The effect of temperature on the current in 0.2 M sulphuric acid with 8 g/l iron in solution.

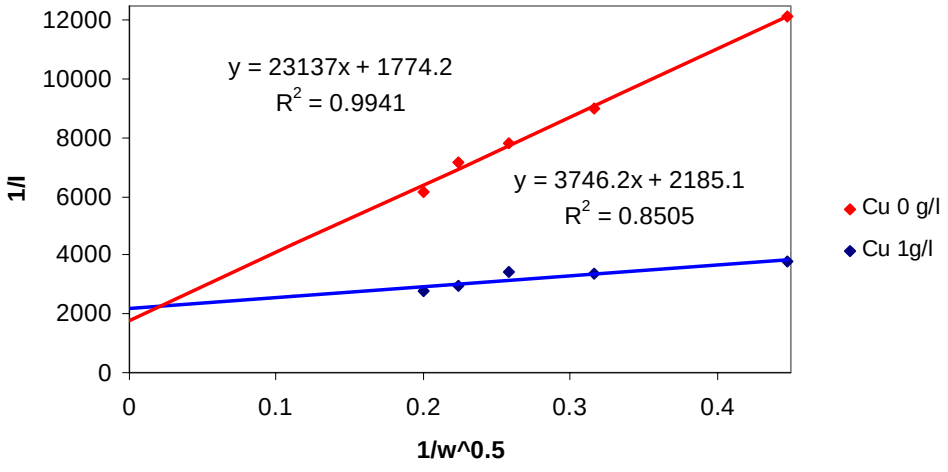

Figure 23. The inverse of the ring current as a function of the square root of the angular speed. The effect of copper on the current in 0.2 M sulphuric acid with 8 g/l iron in solution at 80 °C.

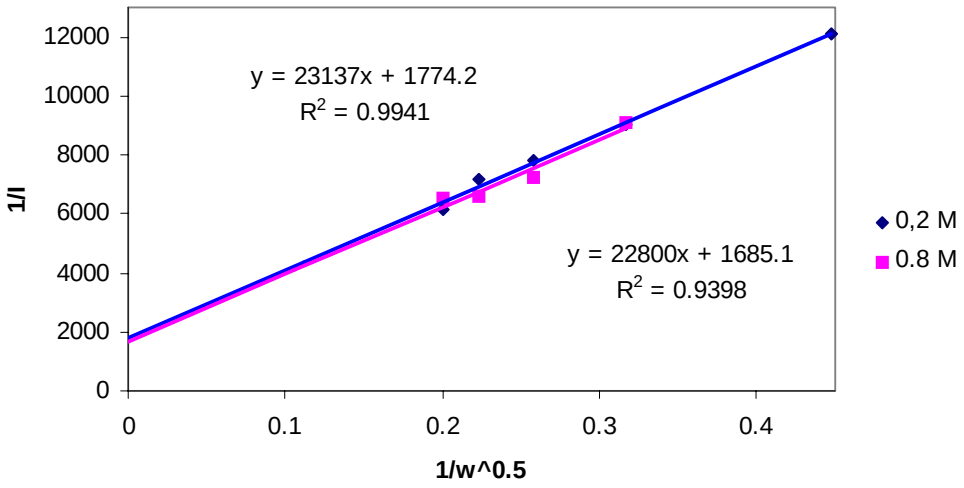

Figure 24. The inverse of the ring current as a function of the square root of the angular speed. The effect of acid concentration on the current in M solutions with 8 g/l iron in solution at 80 °C.

The collector efficiency [62] for the used electrode geometry was 0.19, which means that only 19 % of the ferrous ions formed on the disc electrode were detected on the ring electrode. This had to be taken into consideration when calculating the currents of the disc electrode. Another fact to consider was that the calculated area of the pellet was not the actual area of the sphalerite surface, since the sulphur used as a binder covered part of the surface. No chemical surface analysis was made to analyse the extent of the sulphur coverage, but it must be recognised, that the calculated rates of reaction per area are lower than the actual rates on the concentrate surface. Table 5 shows the rates of reaction at the different temperatures. The rates per area unit are very low, but the fine ground concentrates have a very large total surface area making the total rate of reaction enough for a commercial process.

Table 5. Rates of the dissolution reaction at different temperatures.

T/C	k/(mmol/cm2*min)
70	0.0016
80	0.0014
90	0.0026

8.4.2 Theoretical considerations

The rate of the kinetically controlled process was calculated in the previous section. If the process is controlled by the rate of mass transfer to the spherical particles, the current can be calculated from equation:

$$i_{diff} = \frac{4FD_o c_o}{r} \qquad (35)$$

where i_{diff} is the diffusion current per area (A/cm^2), D_o the diffusion coefficient of the oxidant, Fe^{3+} (cm^2/s) [63], c_o is the bulk concentration of ferric iron and r is the radius of the dissolving ZnS particle. The equation can be used to study the effect of particle size on the rate of the diffusion current. Figure 25 shows the diffusion-limited current divided by the kinetic current for a solution with 8 or 25 g/l of ferric iron at 80°C. The figure shows, that for particle sizes under 300 µm radius, mass transfer is considerably faster than the kinetics under the conditions studied. Increasing the mass transport in the solution cannot increase the rate of the dissolution process; the conditions have to be made more favourable for faster kinetics.

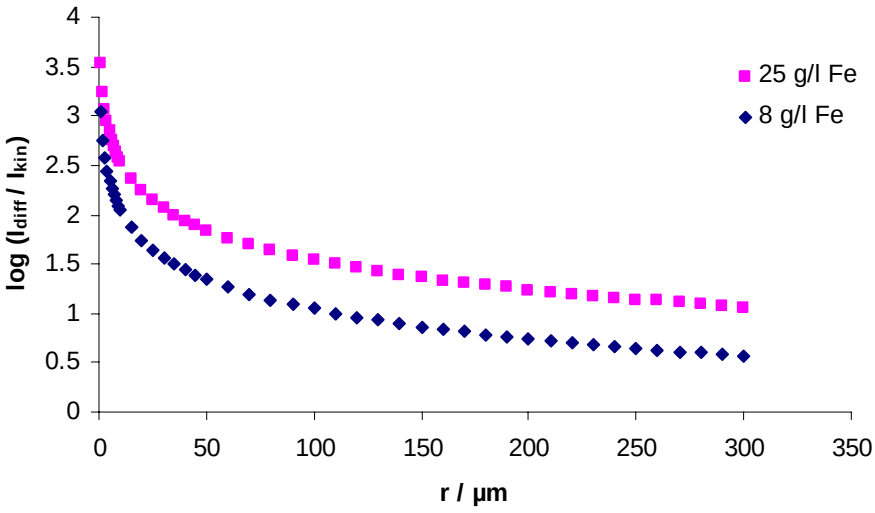

Figure 25. The ratio of the diffusion and kinetic currents as a function of particle radius for sphalerite dissolution in a solution with 8 or 25 g/l of Fe^{3+} in 0.2 M sulphuric acid at 80°C.

9 MINERAL-CARBON PASTE ELECTRODE

The zinc sulphide concentrate does not conduct electricity and thus the potential of the RRDE pellets could not be varied. Conductivity was gained when the concentrate was mixed with fine carbon powder into a paste. The potential of such a mineral-carbon paste electrode can be adjusted and the dissolution rate at different potentials studied. The goal was to have a mineral-carbon paste electrode as the disc on the RRDE set-up.

9.1 MATERIALS

The Concentrate B <37 μm fraction was used. Sulphuric acid solution was diluted from concentrated H_2SO_4 (Merck) with MilliPore ion-exchanged distilled water. The ferric, cuprous and zinc sulphates (Riedel-de Haën) were of reagent grade.

9.2 EQUIPMENT

The mineral-carbon paste electrode was made by mixing the concentrate with finely ground carbon and paraffin oil. The paste was applied to a hole (1 cm^2) in an insulating substrate, with a connection from the paste through the insulation. A schematic of this is shown in picture 26. A standard three-electrode cell was used, with a platinum web as the counter and commercial Ag/AgCl as the reference electrode.

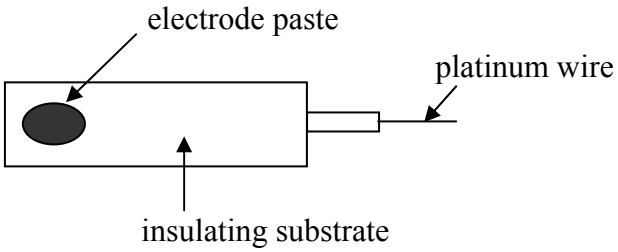

Picture 26. A schematic of the concentrate-carbon paste electrode.

9.3 PROCEDURE

The measurements were conducted at room temperature in an unmixed cell, as the primary target was to study the applicability of the paste electrode. A blank electrode was also constructed with carbon and paraffin oil, so one could be certain the dissolution of the concentrate and not any effects of the paraffin or carbon caused the current. Both potentiostatic and potentiodynamic measurements were conducted. The paste was also incorporated into the RRDE set up as the disc electrode, but it did not seem stable under the applied conditions.

9.4 RESULTS AND DISCUSSION

Figure 27 shows cyclic voltammograms measured on a concentrate-carbon paste electrode in a stationary solution. The figure shows the carbon-oil paste to be inert under these conditions, and thus the current measured on a concentrate-carbon-oil paste was only due to dissolution of the concentrate.

The measurements done on the modified electrode show the effect of the electrode potential on the rate of dissolution. The oxidation reaction began at potentials just below 1 V vs. Ag/AgCl and current flowed as the sulphur in the mineral was first oxidised to elemental sulphur and then further to sulphate according to equations 1 and 4 respectively. Figure 27 also shows a measurement where ferric iron was added to the solution resulting in higher currents at the same potentials as previously. The dissolution was enhanced as some of the sulfide was dissolved by the potential, some by the active iron. On the cathodic sweep the reduction of iron to the ferrous form was seen.

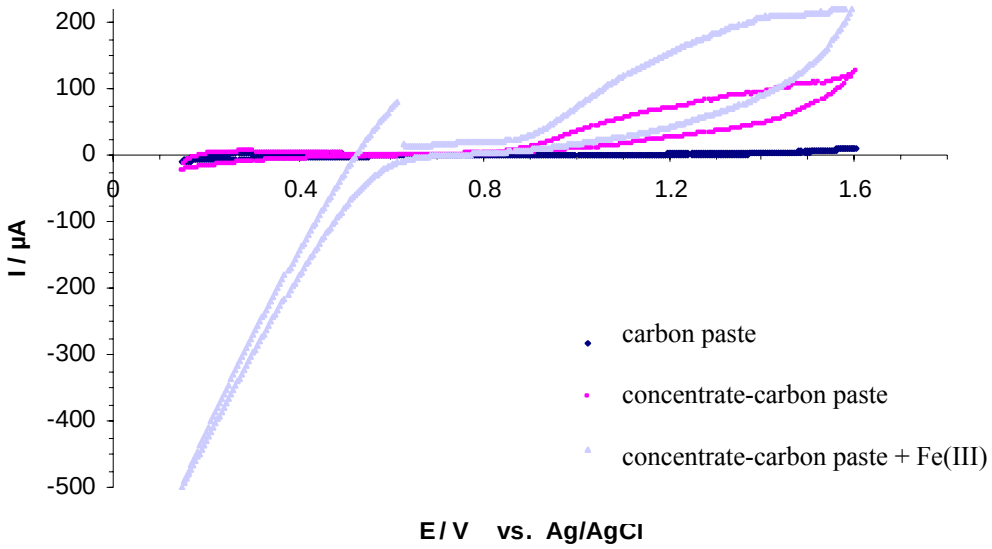

Figure 27. Cyclic voltammograms on a carbon paste- and concentrate-carbon paste -electrode in 0.2 M sulphuric acid solution at room temperature, with 0 or 8 g/l of ferric iron.

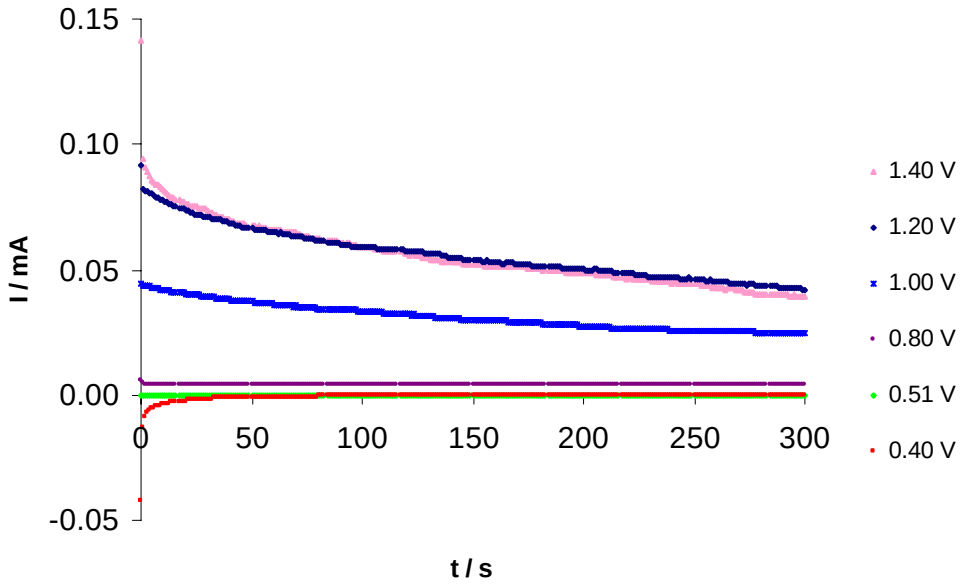

Figure 28. The effect of potential on the current of a concentrate-carbon paste electrode in 0.2 M sulphuric acid at room temperature.

Figure 28 shows the results of potentiostatic measurements, which corroborate the interpretations of the cyclic voltammograms and shows dissolution current as a function of time and potential. As was noted from the cyclic voltammograms, no current passed at potentials under 0.8 V vs. Ag/AgCl and no dissolution occurred. Above this potential dissolution slowly began and the rate was increased with increasing potential until a maximum was reached at 1.2 V vs. Ag/AgCl. As the oxidation current correlates with the rate of sulphur oxidation from the sulphide lattice, the method is suitable for monitoring the reaction rate at various conditions and potentials.

The paste was also incorporated into the RRDE set up as the disc electrode, but the results were not encouraging. The surface area of the RRDE electrode was larger than that of the electrode used for the other CPE measurements and there was a strong flow of solution to the electrode surface. These conditions caused the mineral - carbon paste electrode to be unstable and no useful measurements could be conducted. This problem shall be solved with the optimisation of the paste composition.

10 SUMMARY AND CONCLUSIONS

The dissolution of sphalerite concentrates was studied using ferric ions and manganese dioxide as the oxidant. The methods used were batch dissolution experiments and potentiostatic measurements on a rotating ring-disc electrode with a mineral concentrate disc and on a mineral-carbon paste electrode. The effects of the concentrate fraction size, temperature and the solution iron, zinc and acid concentrations were studied.

In the batch dissolution experiments with manganese dioxide as the oxidant, it was found that MnO_2 affects the dissolution of a sphalerite concentrate (Concentrate A) by two mechanisms: by directly oxidising the sulphur in the mineral and by regenerating the active ferric species. When MnO_2 was the only oxidising species in the solution, the dissolution proceeded linearly with time, which suggests further oxidation of the elemental sulphur layer. This was also suggested by the results showing an excess of MnO_2 dissolution compared to the stoichiometric amount required by the sphalerite oxidation. Analysis of sulphur in the dissolution residue also corroborated the theory of further sulphur oxidation.

The dissolution behaviour of two sphalerite concentrates, Concentrate B and Concentrate C, was studied by batch dissolution experiments using ferric ions as the oxidant. Fractions with particle sizes of less than 37 µm (B1 and C1) and over 37 µm (B2 and C2) were used. The measurement parameters were chosen to match those in industrial scale dissolution. The average conversions for the fractions after 3 hours dissolution were B1: 74 m-%, B2: 74 m-%, C1: 62 m-% and C2: 45 m-%. The conversion of zinc was strongly effected by the size fraction of the concentrate, temperature and the concentration of iron in the solution. The conversions for the smaller concentrate fraction were by average 27 mass percent higher than for the fraction with the larger particle size in the case of the Concentrate B and 21 m-% for the Concentrate C. As expected, the concentrate fraction with the highest specific surface area had the highest conversion and the conversions decreased with decreasing surface area. Once the conversions were

divided by the surface area, the average conversion for the Concentrate C was 15 m-% higher than the one for Concentrate B, which could be due to the increased concentration of iron in the lattice. Increasing the temperature from 80 °C to 95 °C raised the average conversion of the Concentrate B by 15 m-%, the results for the Concentrate C showing only a 3 % increase. The conversion for the Concentrate B was increased by 11 m-% and of the Concentrate C by 7 m-% by the increase of ferric iron from 8 to 25 g/l. The effects of the acid and zinc concentrations were negligible on the conversion.

A rotating ring disc electrode was constructed, in which a pressed concentrate pellet was used as the disc. The Fe^{2+} ions formed by the dissolution of ZnS on the disc surface were detected on the platinum ring by oxidising them back to the ferric form. The measured current was used to determine the rate of dissolution. The method is fast and thus can be used for rapid comparison of the dissolution characteristics of different concentrate fractions under varying conditions. In addition, the method allows for the effects of kinetics and transport processes on the current to be separated, allowing a closer study of the factors affecting the kinetics of the reaction. It was shown, that the reaction mechanism of sphalerite dissolution at 60°C differs from that at higher temperatures and the dissolution rate clearly corresponded to the increase in temperature. The effect of copper on the dissolution kinetics was also evident, while the concentration of the sulphuric acid seemed to have no effect on the rate of dissolution.

Theoretical calculations of the rate of mass transfer showed, that kinetics are rate limiting under these conditions. Increasing the mass transport in the solution will not increase the rate of the dissolution process; the conditions have to be made more favourable for faster kinetics.

A mineral-carbon paste electrode was constructed by mixing the concentrate with fine carbon powder and oil. Cyclic voltammetric measurements showed the carbon-oil paste electrode to be inert under the conditions used. The voltammetric and potentiostatic measurements done on the modified mineral electrode showed

the effect of the electrode potential on the rate of dissolution. The oxidation of the sulphide began above 0.8 V vs. Ag/AgCl and the rate was increased with increasing potential until a maximum was reached at 1.2 V vs. Ag/AgCl. The goal was to have a mineral-carbon paste electrode as the disc on the RRDE set-up; however, the paste used was not stable under the RRDE conditions.

11 REFERENCES

1 Dutrizac, J.E., Pratt, A.R., Chen., T.T., The mechanism of sphalerite dissolution in ferric sulphate-sulphuric acid media, Yazawa International Symposium, Metallurgical and Materials Processing: Principles And Technologies, Vol III: Aqueous and Electrochemical Processings, TMS, 2003.

2 Verbaan, B., Crundwell, F.K., An electrochemical model for the leaching of a sphalerite concentrate, *Hydrometallurgy* **16** (1986) 345-359.

3 Waisener, C.G., Smart, R. St. C., Gerson, A. R., Kinetics and mechanisms of the leaching of low Fe sphalerite, *Geochimica et Cosmochimica Acta*, **67** (5) (2003) 823-830.

4 Bobeck, G., Su, H., The kinetics of dissolution of sphalerite in ferric chloride solution, *Metallurgical Transactions* **16 B** (1985) 413-424.

5 Selvi, S.C., Modak, J.M., Natarajan, K.A., Technical note: Electrobioleaching of sphalerite flotation concentrate, *Minerals Engineering* **11** (8) (1998) 783-788.

6 Owusu, G., Dreisinger, D.B., Peters, E., Effect of surfactants on zinc and iron dissolution rates during oxidative leaching of sphalerite, *Hydrometallurgy* **38** (1995) 315-324.

7 Haung, H.H., Bernal, J.E., Kinetic study on direct leaching of sphalerite in sulfuric acid solution using ferrous sulfate as the catalyst, *Proc. - Electrochem. Soc.* **84-10** (1984) (*Proc. Int. Symp. Electrochem. Miner. Met. Process., 1984)* 469-485.

8 Crundwell, F.K., Kinetics and mechanisms of the Oxidative Dissolution of a Zinc Sulphide Concentrate in Ferric Sulphate Solutions, *Hydrometallurgy* **19** (1987) 227-242.

9 Takala, H., Leaching of zinc concentrates at Outokumpu Kokkola plant, *Erzmetall* **52** (1) (1999) 37-42.

10 Lochmann, J., Pedlik, M., Kinetic anomalities of dissolution of sphalerite in ferric sulfate solution, *Hydrometallurgy* **37** (1995) 89-96.

11 Palencia Perez, I., Dutrizec, J.E., The effect of the iron content of sphalerite on its rate of dissolution in ferric sulphate and ferric chloride media. *Hydrometallurgy* **26** (1991) 211-232.

12 Srinivasan, G.N., Venkatakrishna Iyer, S., Cyclic voltammetric studies on sphalerite electrodes, *Bulletin of Electrochemistry* **16** (1) (2000) 5-9.

13 Lusk, J., Calder, B.O.E., The compostition of sphalerite and associated sulfides in reactions of the Cu-Fe-Zn-S, Fe-Zn-S and Cu-Fe-S systems at 1 bar and temperatures between 250 and 535 °C, *Chemical Geology* **203** (2004) 319-345.

14 Akcil, A., Ciftci, H., Metals recovery from multimetal sulphide concentrates (CuFeS2-PbS-ZnS): combination of thermal process and pressure leaching, *Int. J. Miner. Process.* **71** (2003) 233-246.

15 Han, K. N., Fuerstenau, M., C., Dissolution behavior of metals from binary alloys, Int., J., Process. **72** (2003) 355-364.

16 Palencia, I., Carranza, F., Garcia, M.J., Leaching of Copper-Znic Bulk Sulphide Concnetrate Using an Aqueous Ferric Sulphate Dilute Solution in a Semicontinous System. Kinetics of Dissolution of Zinc, *Hydrometallurgy* **23** (1990) 191-202.

17 Suzuki, I., Microbial leaching of metals from sulfide minerals, *Biotechnology Advances* **19** (2001) 119-132.

18 Fowler, T.A., Crundwell, F.K., Leaching of zinc sulfide by thiobacillus ferrooxidans: bacterial oxidation of the sulfur product layer increases the rate of zinc sulfide dissolution at high concentrations of ferrous ions, *Applied and Environmental Microbiology* **65** (12) (1999) 5285-5292.

19 Long, Z., Huang, Y., Cai, Z., Cong, W., Ouyang, F., Kinetics of continuous ferrous ion oxidation by Acidithiobacillus ferrooxidans immobilized in poly(vinyl alcohol) cryogel carriers, *Hydrometallurgy* **74** (2004) 181-187.

20 Greenwood, N. N., Earnshaw, A., Chemistry of the elements. Pergamon press, Oxford, 1984, 1542.

21 Bard, A. J., Parsons, R., Jordan, J., Standard potentials in aqueous solution. Marcel Dekker, Inc., New York, 1985, 93-110.

22 Lapidus, G., De Lourdes Mosqueira, M., The effect of product solubility on the leaching kinetics of non-porous minerals, *Hydrometallurgy* **20** (1988) 49-64.

23 Jan, R.J., Hepworth, M.T., Fox, V.G., A kinetic study on the pressure leaching of sphalerite, *Metallurgical Transactions B* **7B** (1976) 353-361.

24 Corriou, J.P., Gely, R., Viers, P., Thermodynamic and kinetic study of the pressure leaching of zinc sulfide in aqueous sulfuric acid, *Hydrometallurgy* **21** (1988) 85-102.

25 Dreisinger, D.B., Peters, E., The oxidation of ferrous sulphate by molecular oxygen under zinc pressure-leach conditions, *Hydrometallurgy* **22** (1989) 101-119.

26 Jones, D.A., Paul, A.J.P., Galvanic interactions between alloys and minerals in sulfuric acid, *Corrosion* **50** (7) (1994) 516-521.

27 Madhuchhanda, M., Devi, N.B., Rao, K.S., Rath, P.C., Paramguru, R.K., Galvanic interaction between sulfide minerals and pyrolusite. *J. Solid State Electrochem*., **4** (2000) 189-198.

28 Srinivasa Rao, K., Paramguru, R. K., Dissolution of sphalerite (ZnS) in acidic ferric sulfate solution in the presence of manganese dioxide, *Minerals & Metallurgical Processing* **15** (1), (1998), 29-34.

29 Bard, A. J., Parsons, R., Jordan, J., Standard potentials in aqueous solution. Marcel Dekker, Inc., New York, 1985, 429-439.

30 Mortimer, R.G., *Physical Chemistry*, The Benjamin/Cummings Publishing Company, Inc., New York 1993, 977-984.

31 Munoz, Miller, Wadsworth, Reaction mechanism for the acid ferric sulfate leaching of chalcopyrite, *Met. Trans.* **10 B** (1979) 149-158.

32 Halavaara, P., *Sinkkirikasteen liukenemisnopeuteen vaikuttavat tekijät*, Diplomityö, Lappeenrannan Teknillinen Korkeakoulu, Kemiantekniikan Osasto, Lappeenranta 1996, 70 p.

33 Gramain, P., Thomann, J. M., Gumpper, M., Voegel, J. C., Dissolution kinetics of human enamel powder, I. Stirring effects and surface calsium accumulation, *Journal of Colloid and Interface Science*, **128** (2) (1989) 370-381.

34 Hsu, J-P., Lin, M-J., Dissolution of solid particles in liquids, *Journal of Colloid and Interface Science*, **141** (1) (1991) 60-66.

35 Hsu, J-P., Liu, B-T., Dissolution of spherical particles in liquids, *Journal of Colloid and Interface Science*, **144** (2), (1991) 297-599.

36 Crundwell, F.K., The influence of electronic structure of solids on the anodic dissolution and leaching of semiconducting sulphide minerals, *Hydrometallurgy* **21** (1988) 155-190.

37 Weisener, C. G., Smart, R., St.C., Gerson, A R., A comparison of the kinetics and mechanism of acid leaching of sphalerite containing low and high concentrations of iron, *Int. J. Miner. Process*. **71** (2004) 239-249.

38 Kammel, R., Pawlek, F., Simon, M., Xi-Ming, L., Oxidizing leaching of sphalerite under atmospheric pressure, *Metall* **41** (2) (1987) 158-161.

39 Crundwell, F.K., Refractory behaviour of two sphalerite concentrates to dissolution in ferric sulphate solutions, *Hydrometallyrgy* **19** (1987) 253-258.

40 Buckley, A.N., Wouterlood, H.j., Woods, R., The Surface Composition of Natural Sphalerite Under Oxidative Leaching Conditions, *Hydrometallurgy* **22** (1984) 39-56.

41 Balaz, P., Ebert, I., Oxidative leaching of mechanically activated sphalerite, *Hydrometallurgy* **27** (1991) 141-150.

42 Balaz, P., Alacova, A., Achimovicova, M., Ficeriova, J., Godocikova. E., Mechanochemistry in hydrometallurgy of sulphide minerals, *Hydrometallurgy* **77** (2005) 9-17

43 Xiao, Z., Chen, Q., Yin, Z., Hu, H., Zhang, P., Calorimetic studies on leaching of mechanically actic´vated sphalerite in $FeCl_3$ solution, *Thermochimica Acta* **416** (2004) 5-9.

44 Mikhlin, Yu., Tomashevich, Ye., Asanov, Okotrub, A., Effect of surface non-stoichiometry on the dissolution of metal sulfides in *Electrochemistry in mineral and metal processing V*. Proceedings Vol. 2000-14, The Electrochemical Society, USA 2000, 283-292.

45 Nowak, P., Sulfide sulfur transformations in the processes of the oxidation of metal sulfide's surface, *Technol. Chem. Przelomie Wiekow* (2000) 295-298.

46 Aaltonen, M., "*The Electrochemical Dissolution of Zinc Sulphide Concentrates*", Diplomityö, Teknillinen korkeakoulu 2002.

47 Dutrizac, J.E., Monhemius, A.J., Iron control in hydrometallurgy. Ellis Horwood ltd. Chichester 1986. 169-220.

48 Ghosh, M. K., Das, R. P., Biswas, A. K., Oxidative ammonia leaching of sphalerite Part II: Cu(II)-catalyzed kinetics, *Int. J. Miner. Process.,* **70** (2003) 221-234.

49 Toniazzo, V., Mustin, C., Portal, J.M., Humbert, B., Benoit, R., Erre, R., Elemental sulfur at the pyrite surfaces: speciation and quantification, *Applied Surface Science* **143** (1999) 229-237.

50 Tao, D. P., Richardson, P. E., Luttrell, G. H., Yoon, R.-H., Electrochemical studies of pyrite oxidation and reduction using freshly-fractured

electrodes and rotating ring-disc electrodes, *Electrochimica* Acta **48** (2003) 3615-3623.

51 Koch, D.F.A., Electrochemistry of sulfide minerals, in: Bockris, J. O'M., Conway, B. E., *Modern Aspects of Electrochemistry* **10** (1975) 211-237.

52 Srinivasan, A., Varadharaj, A., Venkatakrishna Iyer, S., Characterization of sphalerite concnetrate electrodes, *Bulletin of electrochemistry* **9** (8-10) (1993) 504-508.

53 Pesonen, P., *Sulfidimineraalien liukenemisen sähkökemiallinen diagnosointimetodiikka*, Lisensiaattitutkimus, Teknillinen Korkeakoulu, Materiaali- ja Kalliotekniikan osasto, Espoo 2000, 87 p.

54 Ahlberg, E., Asbjörnsson, J., Carbon paste electrodes in mineral processing: an electrochemical study of sphalerite, *Hydrometallurgy* **36** (1994) 19-37.

55 Zhang, S., Choi, W.K., Torma, A.E., Kinetics of leaching of a zinc sulfide flotation concentrate with $HCl/FeCl_3$ solutions, *Metall* **42** (9) (1988) 881-884.

56 Choi, W-K., Torma A.E., Electrochemical charecterization of a semiconductor ZnS concentrate during oxidative leaching, in: Lakshmann, V.I. (Ed.), *Advanced Materials - Application of Mineral and Metallurgial Processing Principles*. Society for Mining, Metallurgy and Exploration Inc., Littleton, Colorado 1990, p. 95-107.

57 Nava, J. L., Oropeza, M. T., Gonzales, I., Oxidation of mineral species as a function of the anodic potential of zinc concentrate in sulfuric acid, *Journal of the Electrochemical Society,* **151** (7) (2004) B387-B393.

58 Mikhlin, Y. L., Tomashevich, Y. V., Asanov, I. P., Okotrub, A. V., Varnek, V. A., Vyalikh, D. V., Spectroscopic and electrochemical characterization of the surface layers of chacopyrite ($CuFeS_2$) reacted in acidic solutions, *Applied Surface Science*, **225** (2004) 395-409.

59 Chernyshova, I. V., An in situ FTIR study of galena and pyrite oxidation in aqueous solution, *Journal of Electroanalytical Chemistry* **558** (2003) 83-98.

60 Shapter, J. G., Brooker, M. H., Skinner, W. M., Observation of the oxidation of galena using Raman spectroscopy, *Int. J. Miner. Process* **60** (2000) 199-211.

61 Kendelewicz, T., Doyle, C. S., Bostick, B. C., Brown Jr, G. E., Initial oxidation of fractured surfaces of FeS_2 (1 0 0) by molecular oxygen, water vapor, and air, *Surface science* **558** (2004) 80-88.

62 Albery, W. J., Hitchman, M. L., *Ring-disc electrodes*. Oxford University Press, Oxford, 1971, 175p.

63 Newman, J. S., *Electrochemical systems*. Prentice-Hall, Inc., Englewood Cliffs, N. J., 1973, 432p.

Appendix 1 – The results of batch dissolution experiments 1/2

Measurement	Fraction	T (C)	Fe (g/l)	Zn (g/l)	H (g/l)	X (%)
1	B1	80	125	120	80	72.0
2	B1	95	125	120	20	87.5
3	B1	95	40	60	80	83.1
4	B1	95	125	60	20	86.6
5	B1	80	40	60	80	66.7
6	B1	80	40	120	20	63.2
7	B1	95	125	60	80	90.4
8	B1	95	40	120	20	69.7
9	B1	80	125	120	20	75.7
10	B1	80	125	60	80	74.3
11	B1	80	40	120	80	69.3
12	B1	80	40	60	20	62.8
13	B1	80	125	60	20	63.7
14	B1	95	40	60	20	79.5
15	B1	95	40	120	80	78.5
16	B1	95	125	120	80	68.3
17	B2	80	40	120	20	34.8
18	B2	80	40	60	20	41.5
19	B2	80	125	60	20	54.9
20	B2	80	40	60	80	38.6
21	B2	95	40	120	20	57.3
22	B2	80	125	120	20	48.6
23	B2	95	125	60	20	65.9
24	B2	95	40	60	20	26.0
25	B2	95	40	60	80	45.7
26	B2	95	125	60	80	62.9
27	B2	95	40	120	80	40.7
28	B2	80	40	120	80	29.8
29	B2	80	125	60	80	39.0
30	B2	95	125	120	20	62.0
31	B2	80	125	120	80	40.7
32	B2	95	125	120	80	64.6
33	C1	80	40	60	20	56.3
34	C1	95	40	60	80	78.4
35	C1	80	125	120	20	62.1
36	C1	95	40	120	20	61.6
37	C1	95	125	60	20	71.8
38	C1	80	125	60	80	63.3
39	C1	80	40	120	80	55.2
40	C1	95	125	120	80	82.5

Appendix 1 – The results of batch dissolution experiments 2/2

Measurement	Fraction	T (C)	Fe (g/l)	Zn (g/l)	H (g/l)	X (%)
41	C1	95	8	60	20	42.3
42	C1	80	25	60	20	68.0
43	C1	80	8	120	20	56.3
44	C1	95	25	120	20	46.4
45	C1	80	8	60	80	50.4
46	C1	95	25	60	80	64.9
47	C1	95	8	120	80	58.2
48	C1	80	25	120	80	70.4
49	C2	95	125	120	20	56.7
50	C2	80	125	60	20	43.1
51	C2	95	40	60	20	42.5
52	C2	80	40	120	20	38.3
53	C2	80	40	60	80	36.2
54	C2	95	125	60	80	48.6
55	C2	95	40	120	80	49.6
56	C2	80	125	120	80	44.2
57	C2	80	8	60	20	41.2
58	C2	95	25	60	20	68.5
59	C2	95	8	120	20	24.3
60	C2	80	25	120	20	32.7
61	C2	95	8	60	80	46.2
62	C2	80	25	60	80	46.2
63	C2	80	8	120	80	64.5
64	C2	95	25	120	80	37.5

Appendix 2 – The effect of particle size – Concentrate B

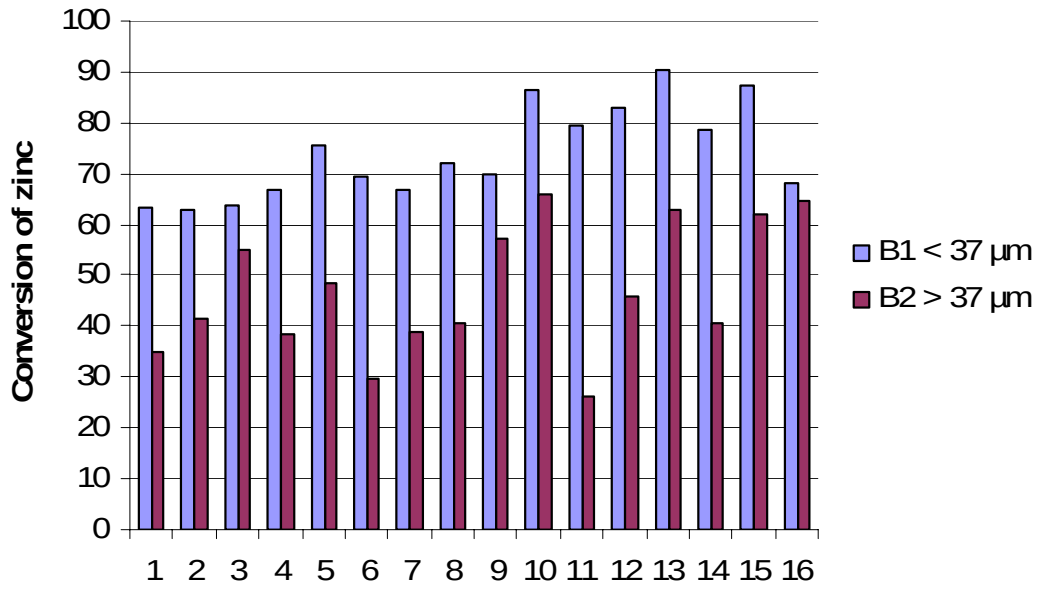

	T/C	Fe(g/l)	Zn(g/l)	H(g/l)
1	80	8	120	20
2	80	8	60	20
3	80	25	60	20
4	80	8	60	80
5	80	25	120	20
6	80	8	120	80
7	80	25	60	80
8	80	25	120	80
9	95	8	120	20
10	95	25	60	20
11	95	8	60	20
12	95	8	60	80
13	95	25	60	80
14	95	8	120	80
15	95	25	120	20
16	95	25	120	80

Appendix 3 – The effect of temperature – Concentrate B

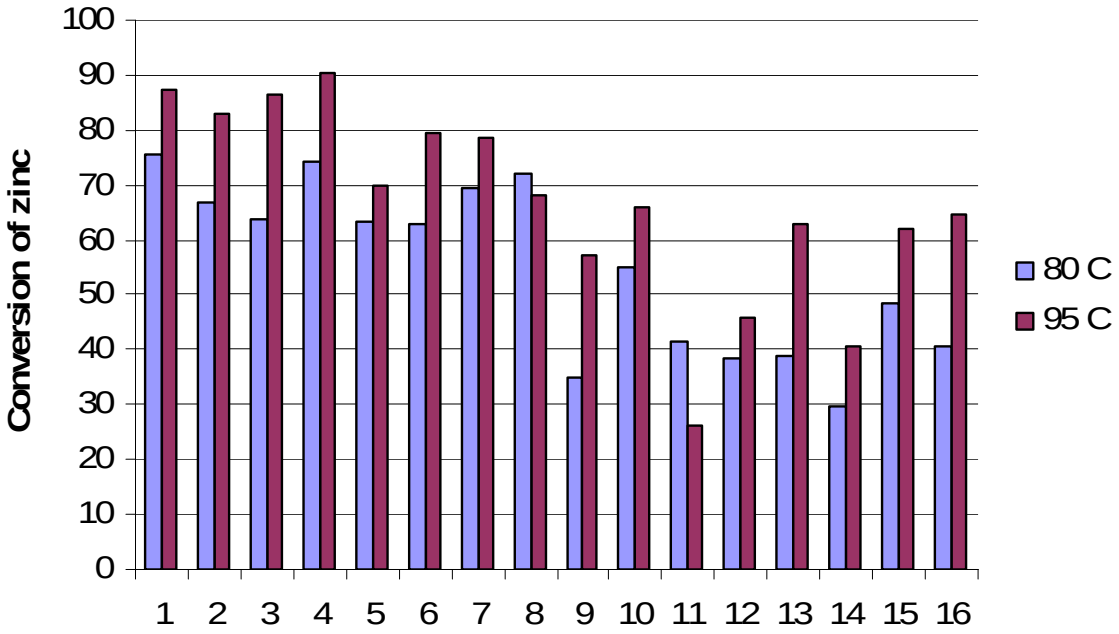

	Fe(g/l)	Zn(g/l)	H(g/l)	Fraction
1	25	120	20	B1
2	8	60	80	B1
3	25	60	20	B1
4	25	60	80	B1
5	8	120	20	B1
6	8	60	20	B1
7	8	120	80	B1
8	25	120	80	B1
9	8	120	20	B2
10	25	60	20	B2
11	8	60	20	B2
12	8	60	80	B2
13	25	60	80	B2
14	8	120	80	B2
15	25	120	20	B2
16	25	120	80	B2

Appendix 4 – The effect of iron concentration – Concentrate B

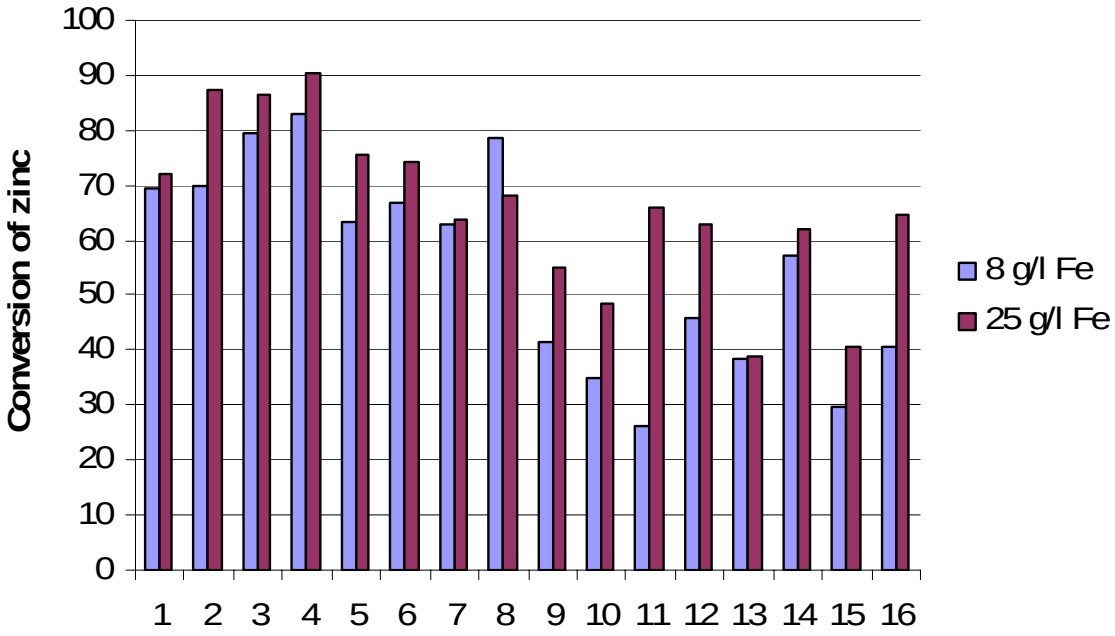

	T/C	Zn(g/l)	H(g/l)	Fraction
1	80	120	80	B1
2	95	120	20	B1
3	95	60	20	B1
4	95	60	80	B1
5	80	120	20	B1
6	80	60	80	B1
7	80	60	20	B1
8	95	120	80	B1
9	80	60	20	B2
10	80	120	20	B2
11	95	60	20	B2
12	95	60	80	B2
13	80	60	80	B2
14	95	120	20	B2
15	80	120	80	B2
16	95	120	80	B2

Appendix 5 – The effect of zinc concentration – Concentrate B

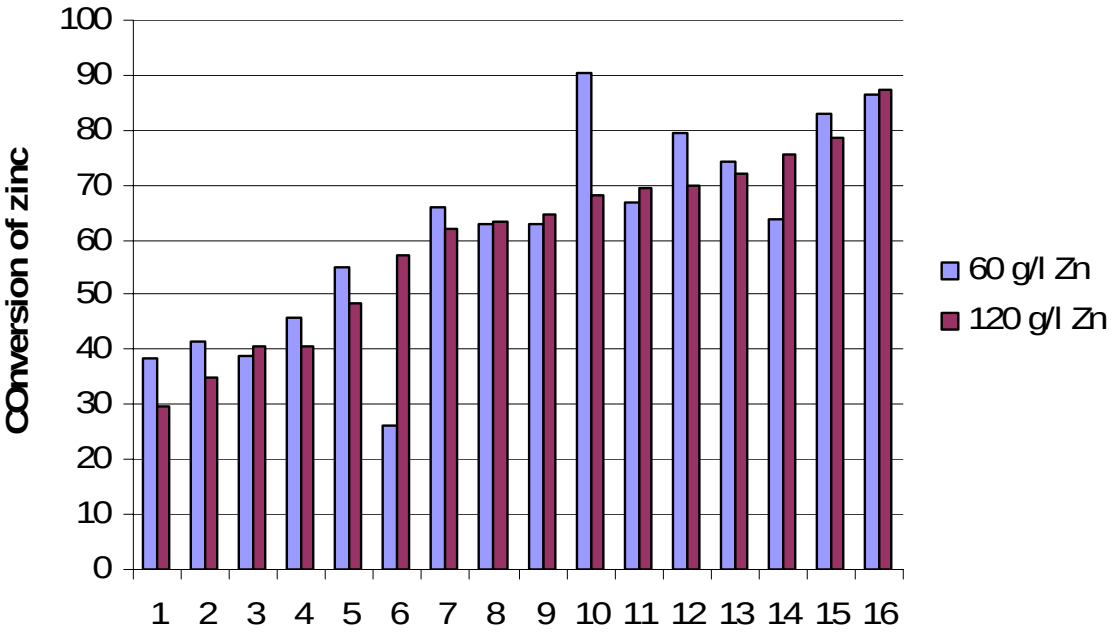

	T/C	Fe(g/l)	H(g/l)	Fraction
1	80	8	80	B2
2	80	8	20	B2
3	80	25	80	B2
4	95	8	80	B2
5	80	25	20	B2
6	95	8	20	B2
7	95	25	20	B2
8	80	8	20	B1
9	95	25	80	B2
10	95	25	80	B1
11	80	8	80	B1
12	95	8	20	B1
13	80	25	80	B1
14	80	25	20	B1
15	95	8	80	B1
16	95	25	20	B1

Appendix 6 – The effect of acid concentration – Concentrate B

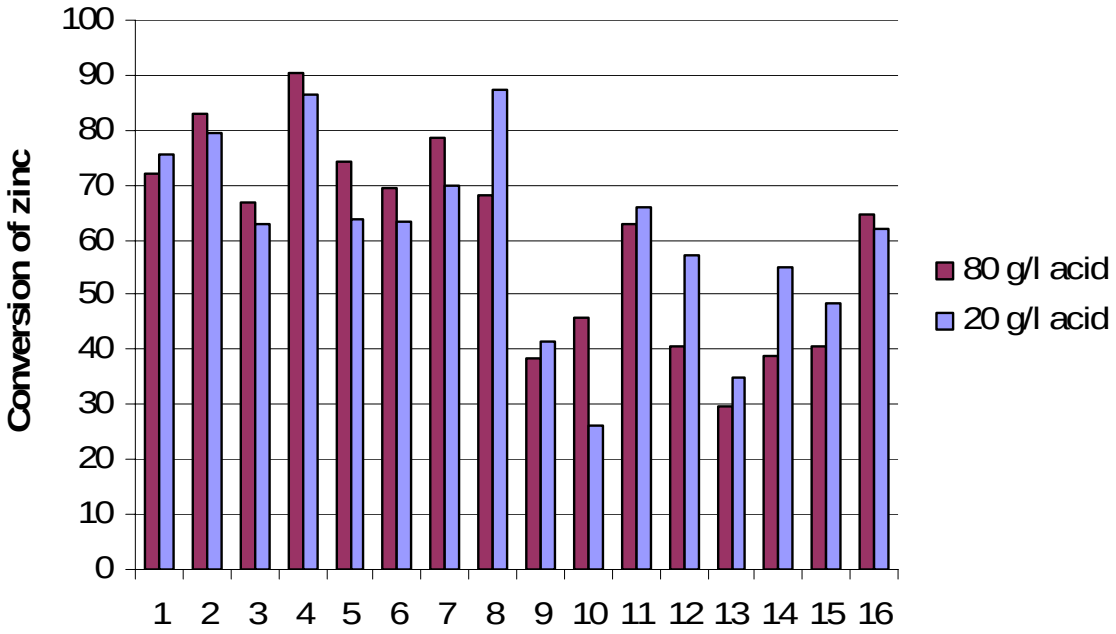

	T/C	Fe(g/l)	Zn(g/l)	Fraction
1	80	25	120	B1
2	95	8	60	B1
3	80	8	60	B1
4	95	25	60	B1
5	80	25	60	B1
6	80	8	120	B1
7	95	8	120	B1
8	95	25	120	B1
9	80	8	60	B2
10	95	8	60	B2
11	95	25	60	B2
12	95	8	120	B2
13	80	8	120	B2
14	80	25	60	B2
15	80	25	120	B2
16	95	25	120	B2

Appendix 7 – The effect of particle size – Concentrate C

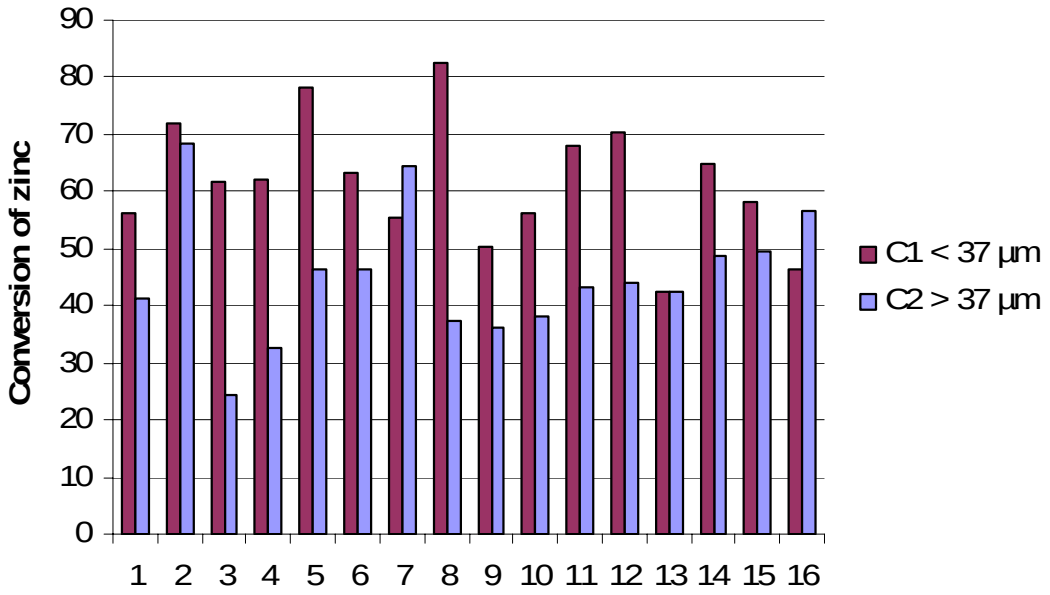

	T/C	Fe(g/l)	Zn(g/l)	H(g/l)
1	80	8	60	20
2	95	25	60	20
3	95	8	120	20
4	80	25	120	20
5	95	8	60	80
6	80	25	60	80
7	80	8	120	80
8	95	25	120	80
9	80	8	60	80
10	80	8	120	20
11	80	25	60	20
12	80	25	120	80
13	95	8	60	20
14	95	25	60	80
15	95	8	120	80
16	95	25	120	20

Appendix 8 – The effect of temperature – Concentrate C

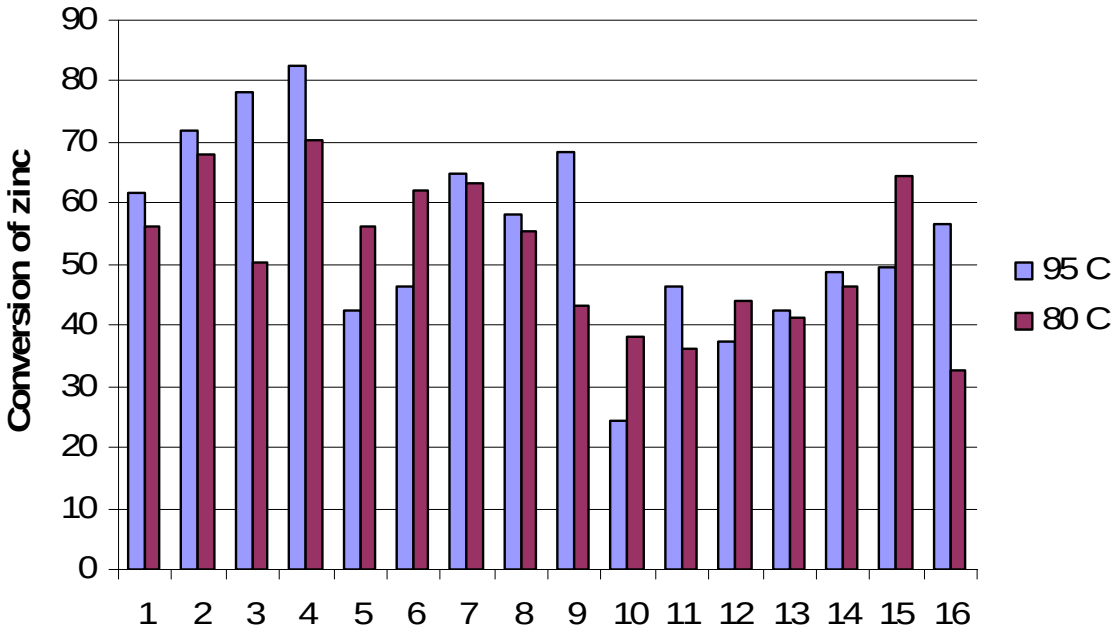

	Fe(g/l)	Zn(g/l)	H(g/l)	Fraction
1	8	120	20	C1
2	25	60	20	C1
3	8	60	80	C1
4	25	120	80	C1
5	8	60	20	C1
6	25	120	20	C1
7	25	60	80	C1
8	8	120	80	C1
9	25	60	20	C2
10	8	120	20	C2
11	8	60	80	C2
12	25	120	80	C2
13	8	60	20	C2
14	25	60	80	C2
15	8	120	80	C2
16	25	120	20	C2

Appendix 9 – The effect of iron concentration – Concentrate C

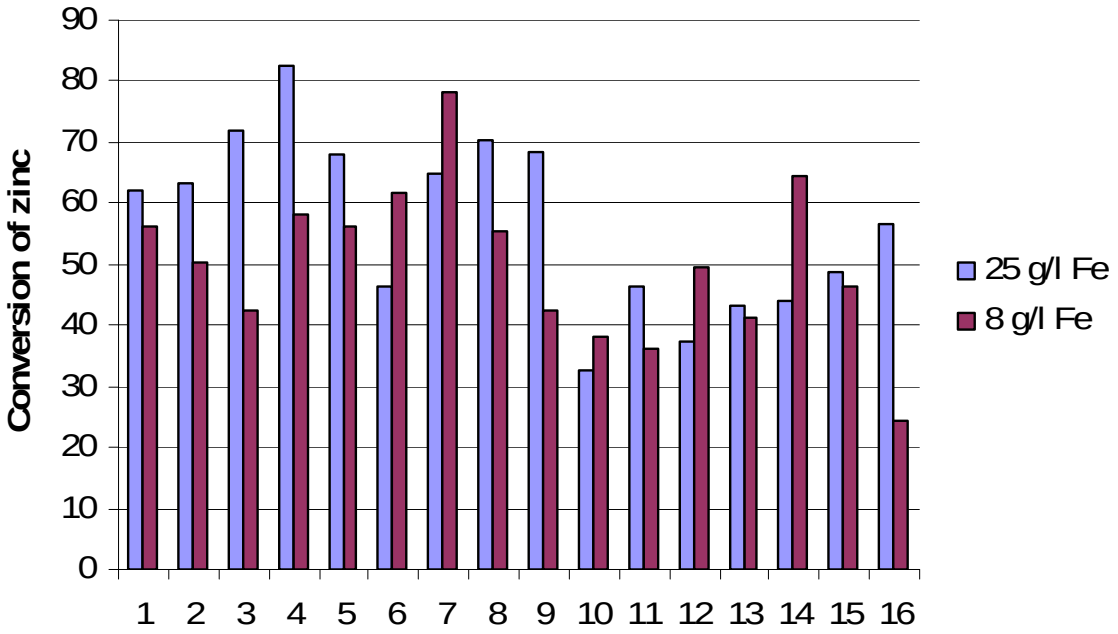

	T/C	Zn(g/l)	H(g/l)	Fraction
1	80	120	20	C1
2	80	60	80	C1
3	95	60	20	C1
4	95	120	80	C1
5	80	60	20	C1
6	95	120	20	C1
7	95	60	80	C1
8	80	120	80	C1
9	95	60	20	C2
10	80	120	20	C2
11	80	60	80	C2
12	95	120	80	C2
13	80	60	20	C2
14	80	120	80	C2
15	95	60	80	C2
16	95	120	20	C2

Appendix 10 – The effect of zinc concentration – Concentrate C

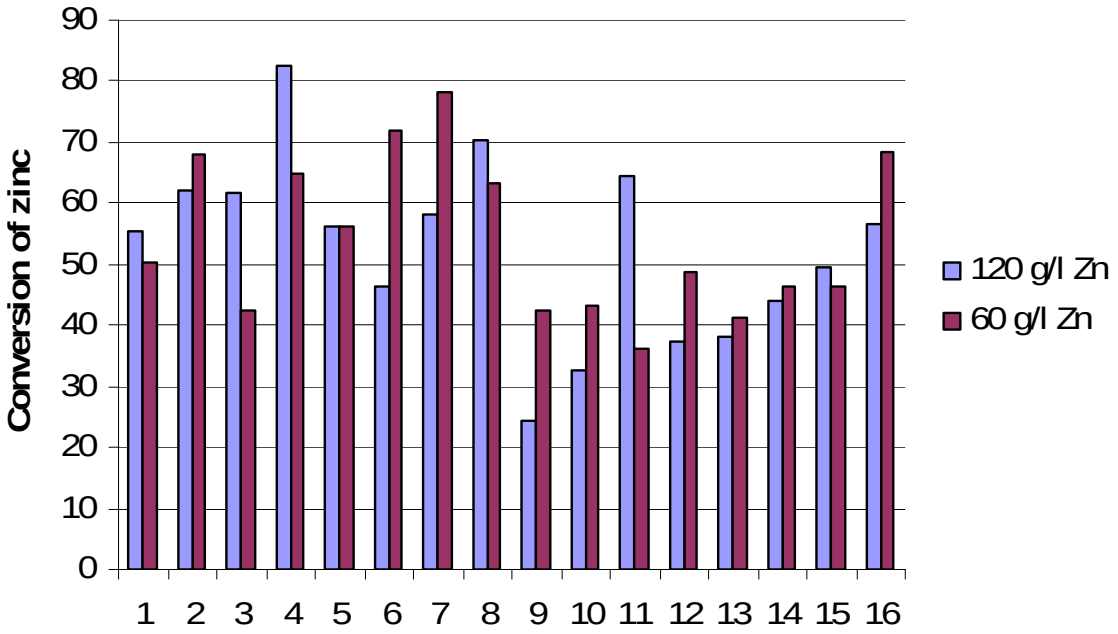

	T/C	Fe(g/l)	H(g/l)	Fraction
1	80	8	80	C1
2	80	25	20	C1
3	95	8	20	C1
4	95	25	80	C1
5	80	8	20	C1
6	95	25	20	C1
7	95	8	80	C1
8	80	25	80	C1
9	95	8	20	C2
10	80	25	20	C2
11	80	8	80	C2
12	95	25	80	C2
13	80	8	20	C2
14	80	25	80	C2
15	95	8	80	C2
16	95	25	20	C2

Appendix 11 – Effect of acid concentration – Concentrate C

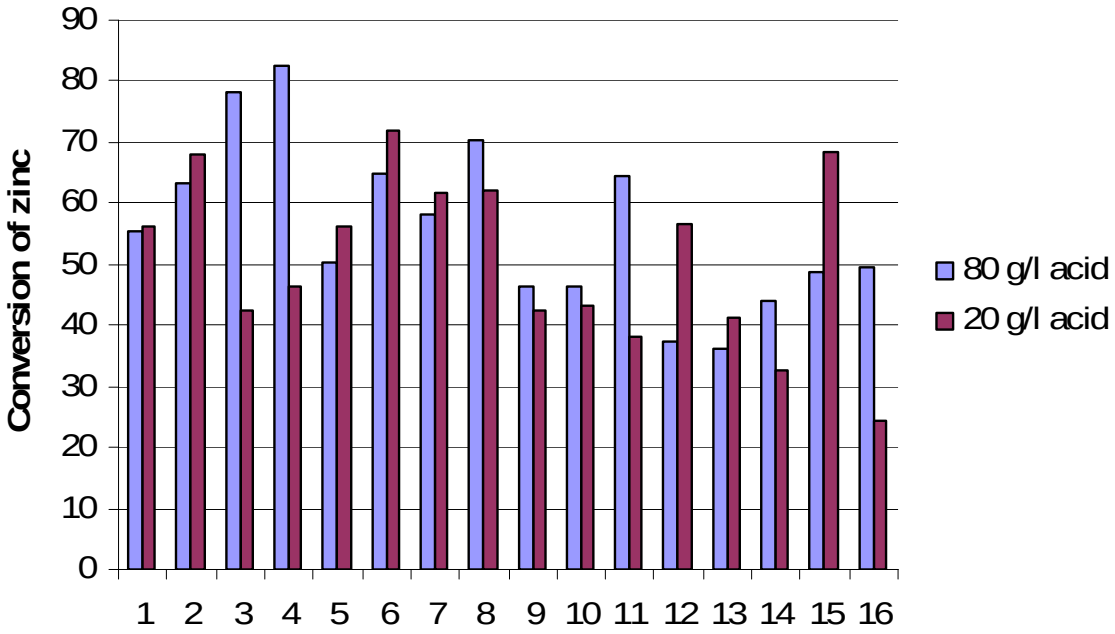

	T/C	Fe(g/l)	Zn(g/l)	Fraction
1	80	8	120	C1
2	80	25	60	C1
3	95	8	60	C1
4	95	25	120	C1
5	80	8	60	C1
6	95	25	60	C1
7	95	8	120	C1
8	80	25	120	C1
9	95	8	60	C2
10	80	25	60	C2
11	80	8	120	C2
12	95	25	120	C2
13	80	8	60	C2
14	80	25	120	C2
15	95	25	60	C2
16	95	8	120	C2

Appendix 12 – Conversions of B1, B2, C1 and C2

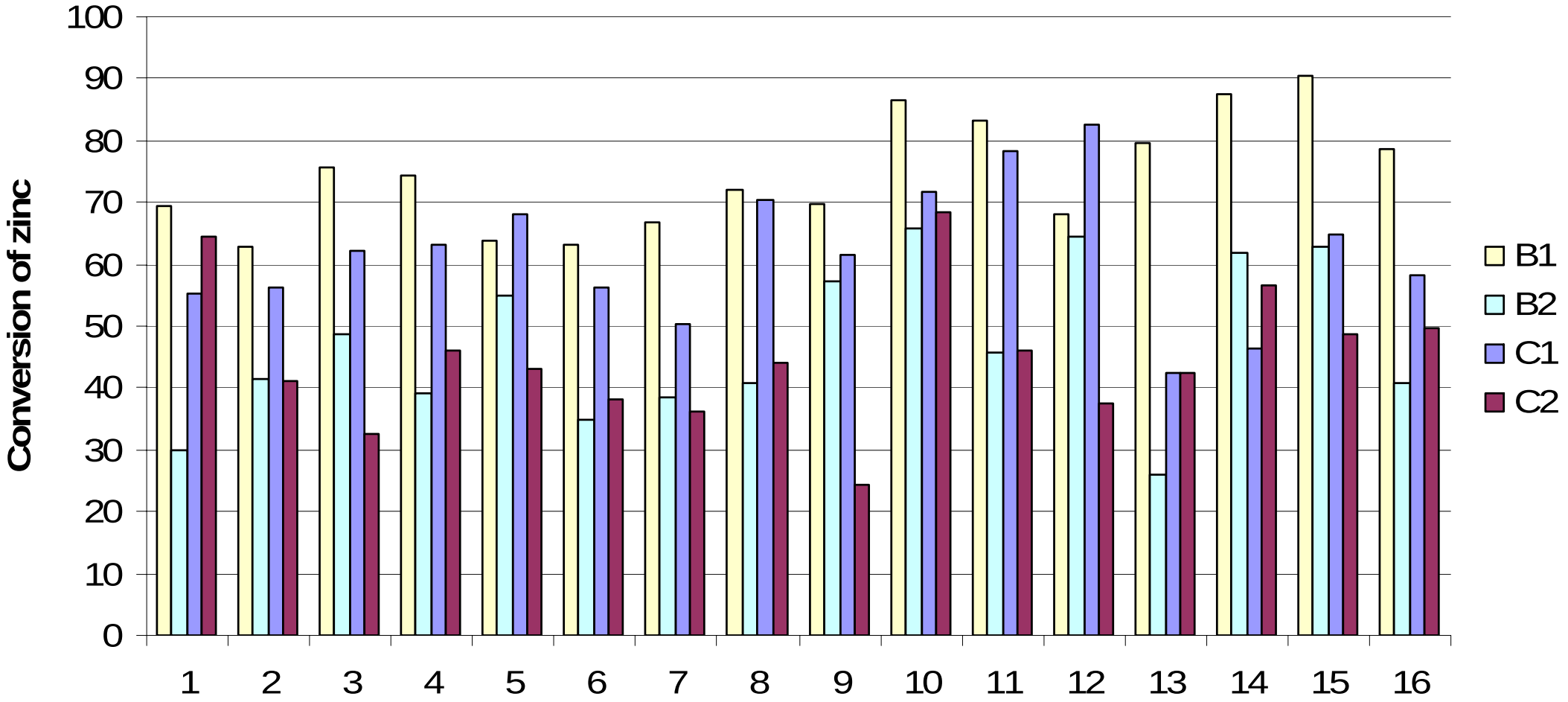

Appendix 13- The repeatability of measurements – Concentrate C

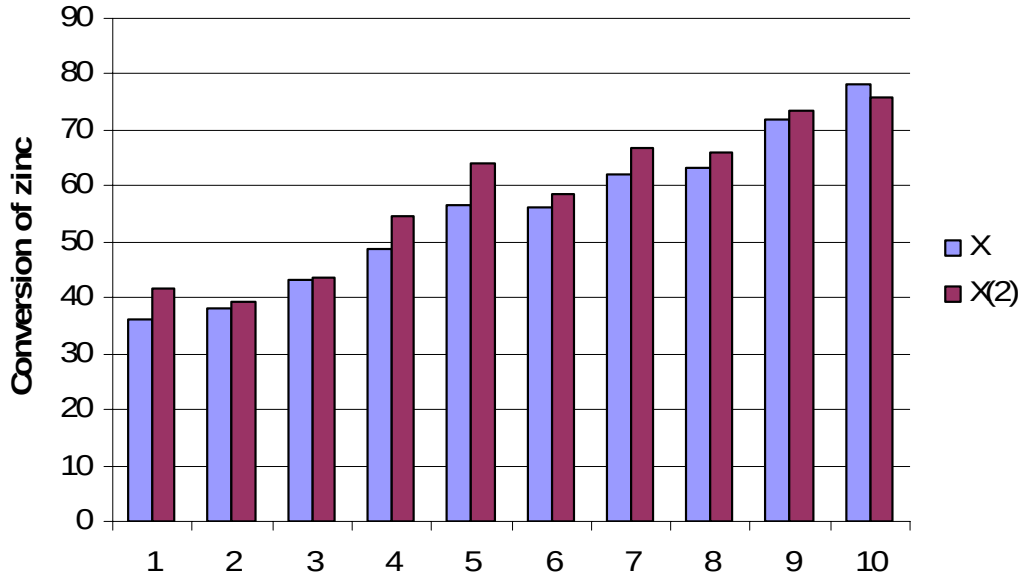

Fr	T/C	Fe(g/l)	Zn(g/l)	H(g/l)
C2	80	8	60	80
C2	80	8	120	20
C2	80	25	60	20
C2	95	25	60	80
C2	95	25	120	20
C1	80	8	60	20
C1	80	25	120	20
C1	80	25	60	80
C1	95	25	60	20
C1	95	8	60	80

Appendix 14- Pictures of the RRDE-pellet before, during and after measurement